Distribution Agreement

In presenting this thesis or dissertation as a partial fulfillment of the requirements for an advanced degree from Emory University, I hereby grant to Emory University and its agents the non-exclusive license to archive, make accessible, and display my thesis or dissertation in whole or in part in all forms of media, now or hereafter known, including display on the world wide web. I understand that I may select some access restrictions as part of the online submission of this thesis or dissertation. I retain all ownership rights to the copyright of the thesis or dissertation. I also retain the right to use in future works (such as articles or books) all or part of this thesis or dissertation.

Signature:

_____ _____

Date

Parallel evolution of alternate morphotypes of *Chryseobacterium gleum* during experimental evolution with *Caenorhabditis elegans*

By

Marissa Duckett Master of Science

Population Biology, Ecology, and Evolution

Nic Vega

Advisor

Joanna Goldberg

Committee Member

Levi Morran

Committee Member

Daniel Weissman

Committee Member

Accepted:

Kimberly Jacob Arriola, Ph.D., MPH

Dean of the James T. Laney School of Graduate Studies

Date

Graduate Division of Biological and Biomedical Science

Population Biology, Ecology, and Evolution

Parallel evolution of alternate morphotypes of *Chryseobacterium gleum* during experimental evolution with *Caenorhabditis elegans*

By

Marissa Duckett

B.S., University of Kansas, 2020

Advisor: Nic Vega, Ph.D. Assistant

Professor of Biology, Emory University

An abstract of

A thesis submitted to the Faculty of the James T. Laney School of Graduate Studies of Emory University in partial fulfillment of the requirements for the degree of

Master of Science

in

Population Biology, Ecology, and Evolution

2023

Abstract

Parallel evolution of alternate morphotypes of *Chryseobacterium gleum* during experimental evolution with *Caenorhabditis elegans*

By Marissa Duckett

Microbial communities shape every organism and environment, and shifts in these communities can cause systemic change within a host that can ultimately affect host health. Understanding how multiple species evolve under the influence of each other in contrast to independently is important for acquiring insight into evolution of community composition, and vice versa. Evolution of community composition is not well understood, but previous research has revealed that community composition converges over evolutionary time. In this investigation, twelve slightly variable communities were created and followed over ten passages in *Caenorhabditis elegans* hosts. Upon the sixth passage, variable morphotypes were observed and maintained as the experiment progressed. We aim to understand what selective pressures could have contributed to this differentiation and maintenance of variable morphotypes. *Chryseobacterium gleum* had the greatest relative abundance in these host associated communities and developed alternate morphologies in two of the twelve communities. Common phenotypes, growth rate, carrying capacity, and motility were measured in hopes of revealing causes for this morphotype differentiation. Growth rate and carrying capacity suggest adaptation to the environment rather than evolution to the inside of the host. Motility was a more useful gauge for variability in these morphotypes, revealing consistently less spread in alternate morphs than original morphs. Gliding motility was confirmed through genomics, but no variability was observed in genetic elements responsible for gliding motility, the Gld proteins and T9SS genes, between alternate, original, and ancestral isolates. Previous research observed an increase in motility as nutrient concentration decreased. Our results did not show this trend, indicating that there are differences in how motility is regulated in *Chryseobacterium*. Although community composition converges over time, microbial lineages evolve differently, likely due to adaptation to environment and regulatory differences in response to unknown selective pressures.

Parallel evolution of alternate morphotypes of *Chryseobacterium gleum* during experimental evolution with *Caenorhabditis elegans*

By

Marissa Duckett

B.S., University of Kansas, 2020

Advisor: Nic Vega, Assistant Professor

A thesis submitted to the Faculty of the James T. Laney School of Graduate Studies of Emory University in partial fulfillment of the requirements for the degree of

Master of Science

in

Population Biology, Ecology, and Evolution

2023

Table of Contents

Introduction

Microbial communities exist in environmental and organismal settings, and researchers consistently observe that microbial communities are variable. Community structure is influenced by the environment that the community inhabits (Estrela et al. 2021). Selective pressures based on environment shape community structure on a metabolic scale (Louca et al. 2018). Partly as a result of these differences in environment, communities differ in composition from one another – for example, the gut microbiome is dissimilar from a soil microbiome only containing 10% as much biodiversity as soil (Blum, Zechmeister-Boltenstern, and Keiblinger 2019). Soil microbiomes and the human gut microbiome vary in several environmental characteristics and their microbiomes reflect that (Rinninella et al. 2019), (Wei et al. 2019). It is also observed that community composition will vary even between two communities from the same type of location (Louca et al. 2018). For example, the composition of the gut microbiome of two humans will be different (Louca et al. 2018). Microbiomes are also observed to change with time, as the composition of an infant gut is different that of an adult (Avershina et al. 2016).

In experimental evolution, communities of the same initial structure tend to follow similar trends in composition over time. The same or similar taxa are present across communities, which suggests similar selective pressures at some level. However, the specific traits of a given taxon within these communities can be different, even in communities with similar composition and structure. Each bacterium will experience different selective pressures. This selection can generate within-species variability. Species, as a result of this selection, evolve variably in community contexts, resulting in differences in phenotype within and between communities and passages. This species-level evolution shapes community composition and evolution (Taylor and Vega 2021). (Estrela et al. 2021),(Taylor, Janasky, and Vega 2022), (Morella et al. 2019).

Host-associated communities are also observed to evolve to their environment, which is the host. Community composition differences corresponding to host genotypes have been observed, but the importance of host association is still debated (Morella et al. 2019). Host-associated and host-independent communities are both observed to converge in composition over time, revealing community convergence is a staple of community evolution (Chang et al. 2021). Causes of this convergence are still not understood, nor are the selective pressures that cause their fast-slow convergence in various community structures.

Caenorhabditis elegans is a good simple host model for studies of host-associated evolution. Fast host life cycles allow for large numbers of individuals over multiple generations in a short period of time, so host-associated evolution can be observed on a faster time scale. Due to small body size, large numbers, and ease of handling, multiple conditions and/or communities can be run in a single experiment, allowing easy replication of samples and comparison over many conditions within a single run. *C. elegans* is a well-studied host, with a breadth of community composition information published for the gut microbiome (Ford and King 2020).

In this work, we investigate emergence of within-species variation in *C. elegans*-associated communities. During experimental adaptation of minimal communities, we observe emergence of morphological variants in *Chryseobacterium gleum*, which was initially present in half of the starting communities. To attempt to identify the selective pressures that lead to morphological variation, we performed persistence, motility, growth rate, and competition assays of each *Chryseobacterium gleum* morphotype. By assessing variation of phenotypic traits both within- and between-morphotypes, as well as at the community and passage levels, we observed differences in motility, but no consistent selection on this trait. The selective pressure that produced the variation remains unclear. We aim to understand these evolutionary aspects of species variation so that we can make larger-scale generalizations about community structure and emergence of variants.

Results

In this experiment, twelve communities were created and replicated. Each community started off with a slightly different composition, varying at a species level, but from the same genera (see Methods). Each of these communities were experimentally evolved on NGM plates with *C. elegans* for ten passages. Each passage had a 7 day period, after which communities were passaged to fresh plates and a sample of worms was digested and plated to visualize the species composition. Cryo-preservation of samples allowed phenotypic and genotypic comparisons of isolates from different passes and communities to measure the outcomes of selection (Figure 1).

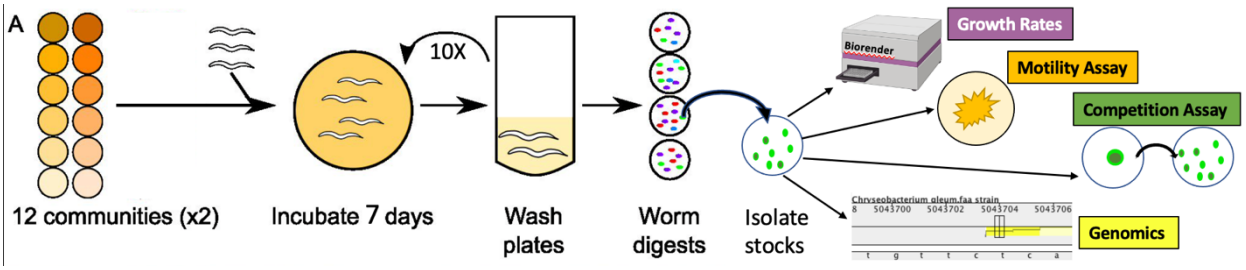

Figure 1 Experimental workflow for community-based evolution. The experimental set up for the previous project consisted of 12 seven member communities, similar at a genus level but variable on a species level. Each community had a replicate made, resulting in A1 and A2 communities and the like. These communities were grown with worms and passaged every seven days to fresh NGM agar plates. Worm digests were conducted to reveal the bacterial community composition. Isolates were picked, this revealed species variability. Isolates reflective of original and alternate morphologies were used in phenotypic variability testing. Growth rates and carrying capacity were measured in a plate reader. Motility assays were conducted on agar plates with variable agar. Competition assays were conducted by growing an alternate and original morph together then plating them, the amount of each morphotype was counted to quantify which was a stronger competitor. Genomics were conducted with specific strains, SNPS and their corresponding genes were identified. The image displays a SNP on a *C. gleum* genome.

As previously observed (Taylor, Janasky, and Vega 2022) experimental passaging of combinatorial bacterial communities with *C. elegans* (Figure 1) resulted in coherent trajectories of community composition (Figure 2). These trajectories were characterized by rapid loss of community richness, resulting in communities comprised almost entirely of *Chryseobacterium gleum/indologenes* (CX), *Microbacterium oxydans* (MO), and *Ochrobactrum anthropi* (OA). Composition of worm gut contents converged to one of two states; communities initiated with *C. gleum* came to be dominated by that species, whereas communities initiated with *C. indologenes* were numerically dominated by *M. oxydans* and *O. anthropi* (Figure 2 C). While this fast-slow pattern in compositional change was also observed in communities passaged without *C. elegans* (Figure 2 A), community composition was very different (Figure 2 B), indicating that the worm played an important role in shaping these communities.

Morphological variants were observed in *Chryseobacterium* and *M. oxydans* beginning around passage 6 of these experiments (Figure 2 D). With some exceptions, variants emerged nearly in synchrony across communities. These variants were detected as novel colony morphologies on nutrient agar plates (Figure 3). Timing of variant emergence in *C. gleum* corresponded with time-series minimums of compositional diversity (Figure 4). Not all communities produced variants; in most cases, only one of a given pair of replicate communities did so. No communities produced variants of both *Chryseobacterium* and *M. oxydans*.

We chose to focus on characterization of within-species diversity in *Chryseobacterium gleum*, which generated two of the three alternate *Chryseobacterium* morphs that persisted over passages 6-10 (Figure 2 E). *C. gleum* alternate morphs were observed in community A replicate 2 and community F replicate 2; the remaining replicate of both communities generated only colonies of the original morphotype. Taxonomy was confirmed via 16S sequencing, and original and alternate morphs of CG both had highest homology matches with *Chryseobacterium cucumeris* XS (*C. gleum* group).

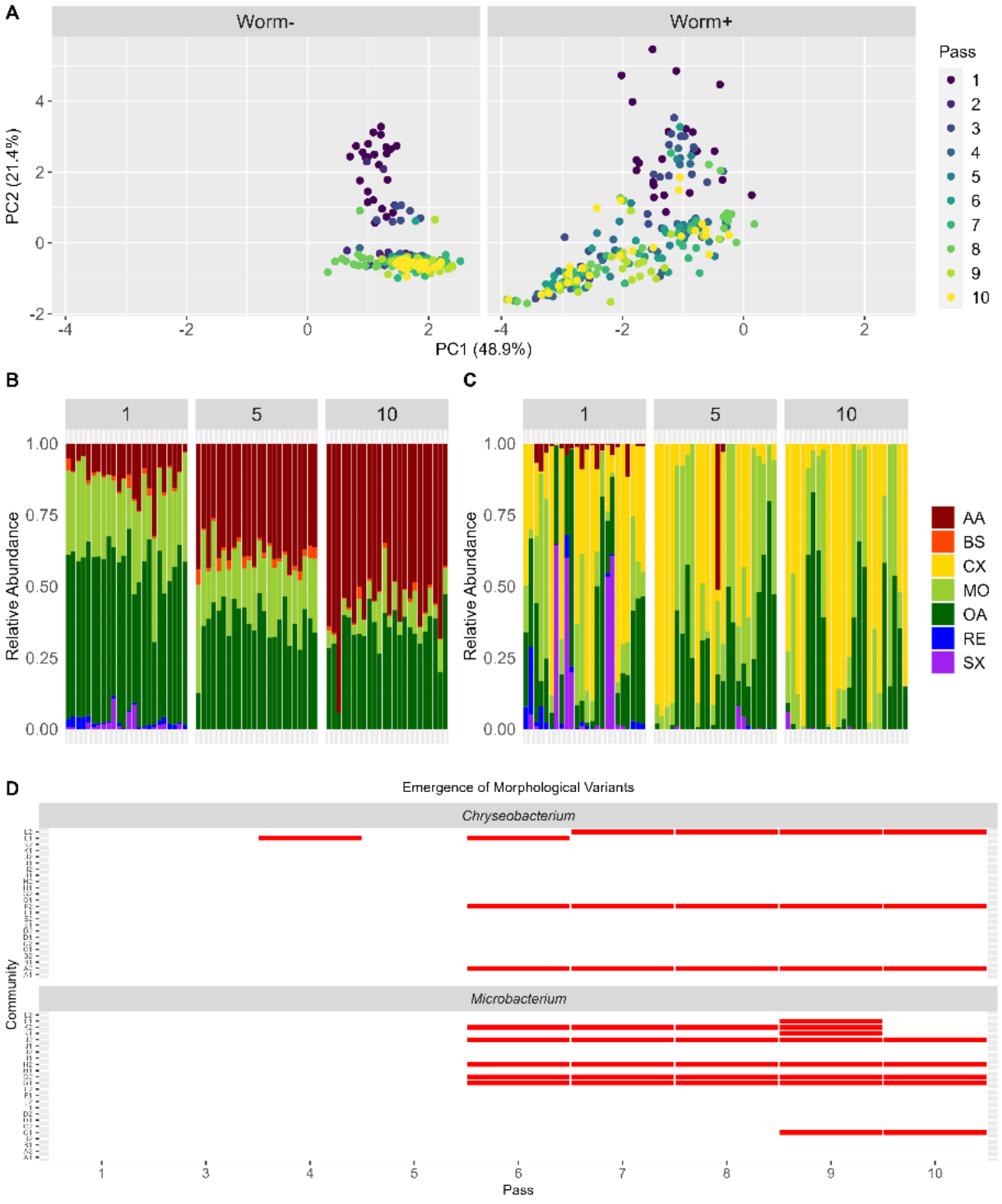
A
Worm-
Worm+
PC2 (21.4%)
PC1 (48.9%)
Pass
1
2
3
4
5
6
7
8
9
10
B
C
1
5
10
Relative Abundance
AA
BS
CX
MO
OA
RE
SX
D
Emergence of Morphological Variants
Chryseobacterium
Microbacterium
Community
Pass

Figure 2 . Community-based adaptation produces convergent community composition along with diversification within and between communities. (A-C) Community composition follows coherent trajectories over time in the presence (right) and absence (left) of *C. elegans*, with compositional differences associated with the presence of worms. For plates with worms (right), data are from batch digests of adult worms taken from plates at the end of each passage (n=50 adult worms per batch). For plates established without worms (left), data are for communities washed from plates. (A) PCA of community composition data over time (ten passages of experimental evolution) Each point represents one replicate (12 communities, two replicates each). (B, C) Relative abundance for communities in passages 1, 5, and 10; each bar represents one replicate as in (A). Communities are shown in order of community ID and replicate number (community A replicate 1, A replicate 2, B replicate 1, B replicate 2…; two replicates for each of 12 communities, n=24 bars). Here "CX" refers to either CG or CI, "RE" refers to RE15D, RE15M, or RE16, and "SX" refers to either SS or ST, according to the starting composition of the individual communities (Table 2). *C. gleum* (CG) is the *Chryseobacterium* isolate in communities A-B, E-F, and I-J (two replicates each: columns 1-4, 9-12, 17-20 out of 24 in panels B-C). (D) Emergence of morphological diversity in worm-associated communities. Community replicates are on the y-axis (in reverse order top to bottom, L2->A1). Passages where two distinct morphotypes were observed for *Chryseobacterium* (top) and *Microbacterium oxydans* (bottom) are marked in red. (Data by Megan Taylor)

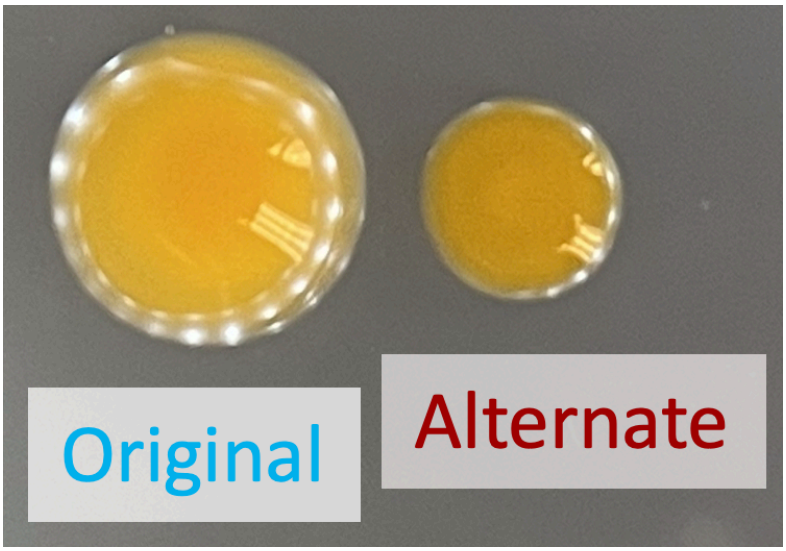

Figure 3. Phenotyping of original (o) and alternate (a) morphs of *C. gleum*, based on distinct phenotypes on salt-free nutrient agar. The original morph is brightly colored, glossy, round, smooth, and slightly mucoid. The alternate morph is smaller and flattened, with less opacity and duller coloration.

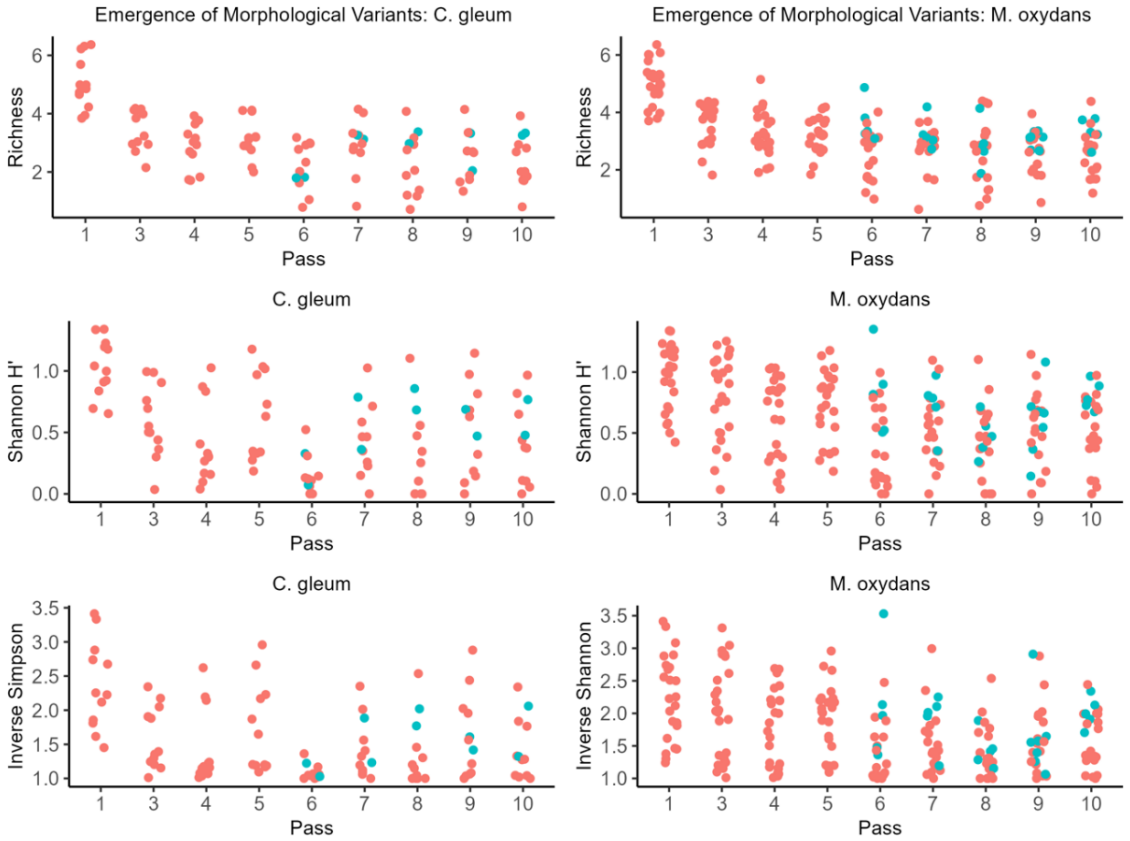

Figure 4. Emergence of alternate morphs of *C. gleum* (left) but not *M. oxydans* (right) coincides with time-series minimums of taxonomic diversity. Each data point represents one of two replicates of each community (n= 12 points for 6 communities containing *C. gleum* and 24 points for 12 communities containing *M. oxydans* at each passage). Communities without alternate morphs are shown in pink; communities with alternate morphs of the indicated species are shown in blue. Each row reports a different measure of community diversity (richness, Shannon H', inverse Simpson). (Data by Megan Taylor)

C. gleum is a worm pathogen

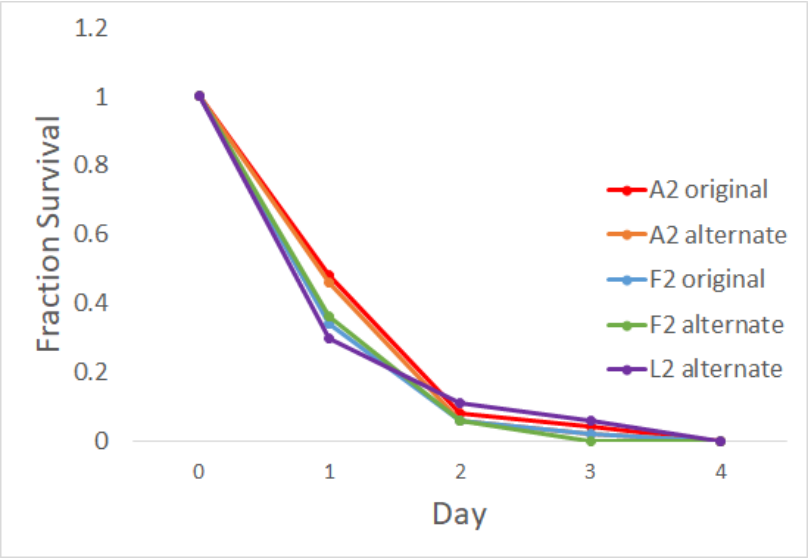

Figure 5. *Chryseobacterium gleum* kills N2 Bristol *C. elegans*. In these assays, day 2 synchronized adult worms (n=100) were added to 6 cm NGM plates with lawns of pass-10 isolates of *C. gleum*. Mortality was assessed at 24 hour intervals. (Data by Megan Taylor)

Community plates initiated with *C. gleum* tended to support small, struggling populations of worms and heavy lawns of bacteria at the end of each passage. In previous work with these communities (Taylor, Janasky, and Vega 2022), we determined that *C. gleum* was pathogenic toward worms. We sought to determine whether pathogenicity was altered during adaptation in these communities, and in particular whether alternate and original morphologies differed in pathogenicity. Survival assays (Figure 5) indicated that pathogenicity of pass-10 *C. gleum* isolates toward worms was very similar across communities and morphologies, indicating that pathogenicity was not substantially altered during adaptation.

There is variability within community and passage and between isolates

Variation was observed within both the original and alternate morphologies. Streaking out individual colony isolates (here, from community F1) revealed variation in pigment, colony size, and mucoid nature (Figure 6).

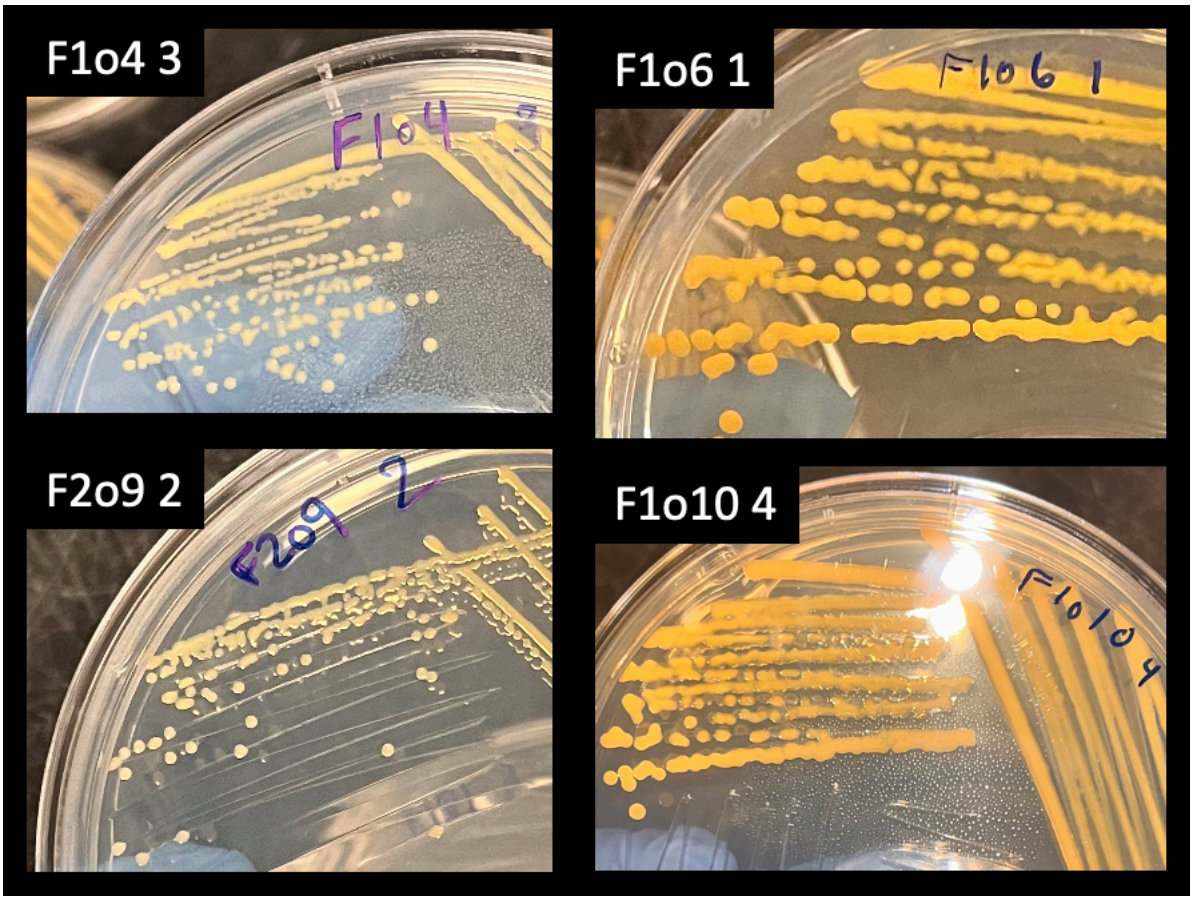

Figure 6. Variation in colony morphology within the "original" morphotype in Community F1, passages 4, 6, 9, and 10. Photos were taken of two-day old nutrient agar plates.

Growth rate is lower and carrying capacity is greater in alternate morphs than ancestor

Growth rate and carrying capacity are traits often selected on in changing environments. We hypothesized that there would be differences in growth rate and/or carrying capacity within and between isolates of *C. gleum* from A1, A2, F1, and F2 communities and passages 6 and 10. This information would help inform what selective pressures contribute to the emergence of alternate morphologies by providing insight into how growth parameters differ between morphotype, passage, and community and ancestral isolates. Alternate morphotypes are rare in the *C. gleum* population. However, growth rate and/or carrying capacity has allowed for a rare morphotype to

coexist with and find a stable fixed point with original morphotypes. Higher exponential growth rate could allow for the rare morphotype to reach carrying capacity more quickly, allowing it to coexist with the dominant morphotypes. Alternatively, a higher carrying capacity and a slow growth rate would allow for an alternate morphotype to be sustained in a system. These examples of stable states could explain the conditions that allowed emergence of alternate morphotypes and resulted in coexistence. Based on the experimental results, it could be asserted that growth rate and/or carrying capacity could be selected for or against in variable communities, and that this differentiation in selection could be a reason for the emergence of alternate morphotypes. To measure growth rate and saturation density under the nutrient conditions in the original environment, individual isolates were grown in liquid NGM for 24 hours in a plate reader, and cultures were dilution plated at the end of the run to determine density in colony forming units (CFU)/mL. This experiment revealed that growth rate was slightly lower in alternate morphs and F2010 than in the ancestral and the remaining original morphs (Figure 7 A). OD600 at saturation was relatively similar across all samples (Figure 7 B), but dilution plates revealed consistently greater carrying capacity in alternate morphs as compared with ancestor (Figure 7 C). Several original morphs (A1010 ($p<=0.01$), A2010 ($p<=0.001$), F106 ($p<=0.01$), and F2010 ($p<=0.05$)) also showed higher saturation density than the ancestor. These results also suggest an increase in carrying capacity over time in original morphs.

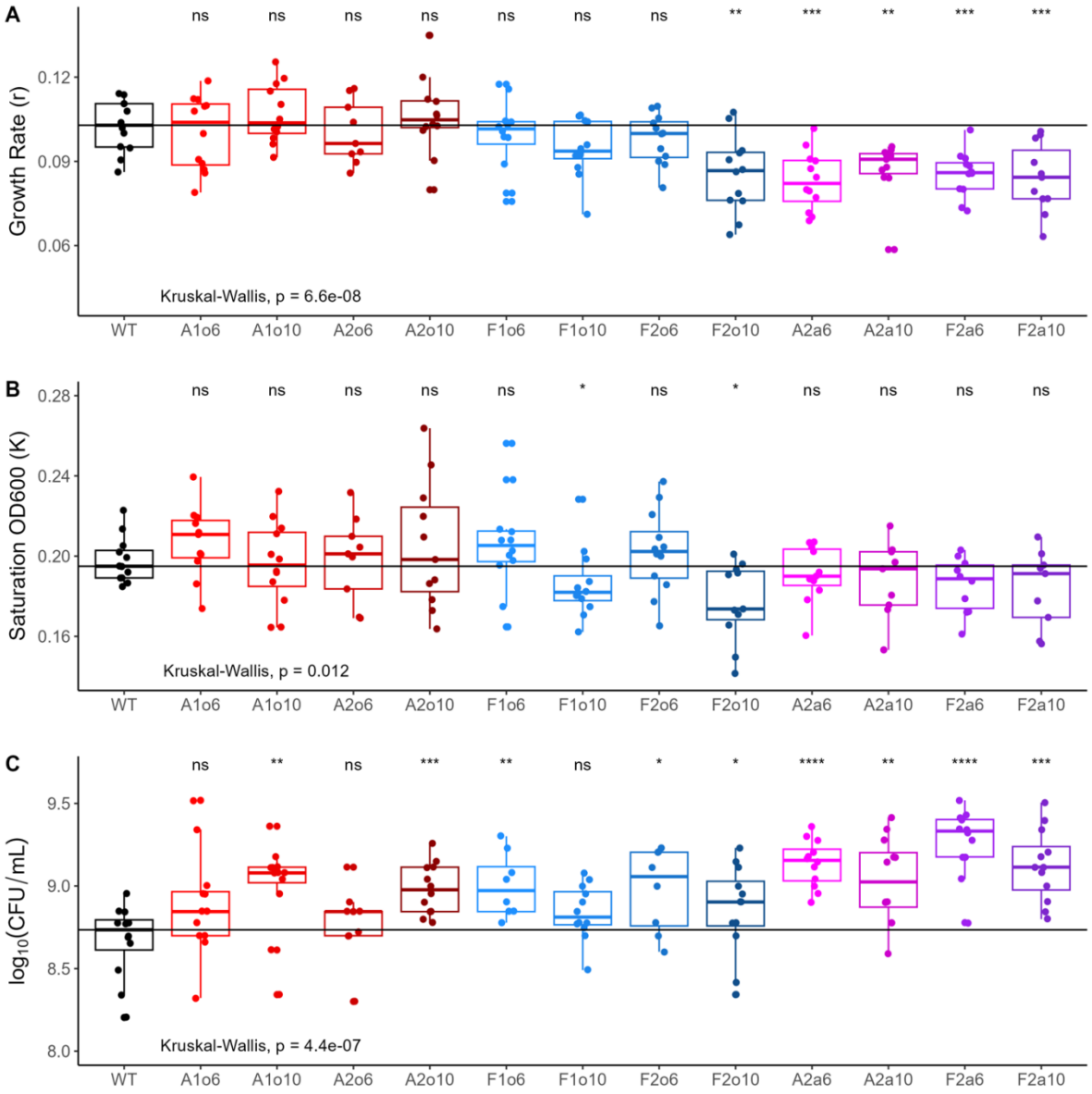

Figure 7. Phenotyping of *C. gleum* original (o) and alternate (a) morphs from communities A and F. Ancestral isolates are shown as "WT". Maximum exponential growth rate (h^{-1}) (A) and OD600 saturation density (B) were estimated from plate reader growth curves in liquid NGM media at 25°C. Saturation density in CFU/mL (C) was estimated by dilution plating the same cultures after 24 hours growth in plate reader. Data represent three independent experiments on separate days, using the same isolates in all runs (n=4 from each community and passage). Results of pairwise Wilcoxon rank sum tests against the ancestor are shown above each data set (*, p<=0.05; **, p<=0.01; ***, p<=0.001; ****, p<=0.0001).

Pairwise competition in vitro

Next, we sought to determine why we observed alternate morphs in one replicate community but not the other. If alternate morphs could not compete successfully against original morphs from communities where morphological diversity was not seen, that would provide an explanation for why alternate morphs were found in some communities/replicates but not others. To assess competitive interactions, we co-cultured alternate and original morphologies on NGM agar with the same seven-day passage window used during experimental evolution and measured the fraction of each morphotype present. We observed that alternate morphs were maintained in all pairwise combinations over time, frequently dominating these populations, and that neither morphotype was excluded in any combination (maximum alternate morph relative abundance 99.45%). Alternate morphs rarely decreased in relative abundance, and sometimes even increased as they were passaged (Figure 8). This indicates that intra-species competitive exclusion does not explain the absence of alternate morphs in communities A1 and F1 (Figure 8). Nor did alternate morphs consistently perform better or worse in competition with original morphs from the same community and passage, indicating no evidence for Red Queen-type arms-race dynamics (Morran et al. 2011).

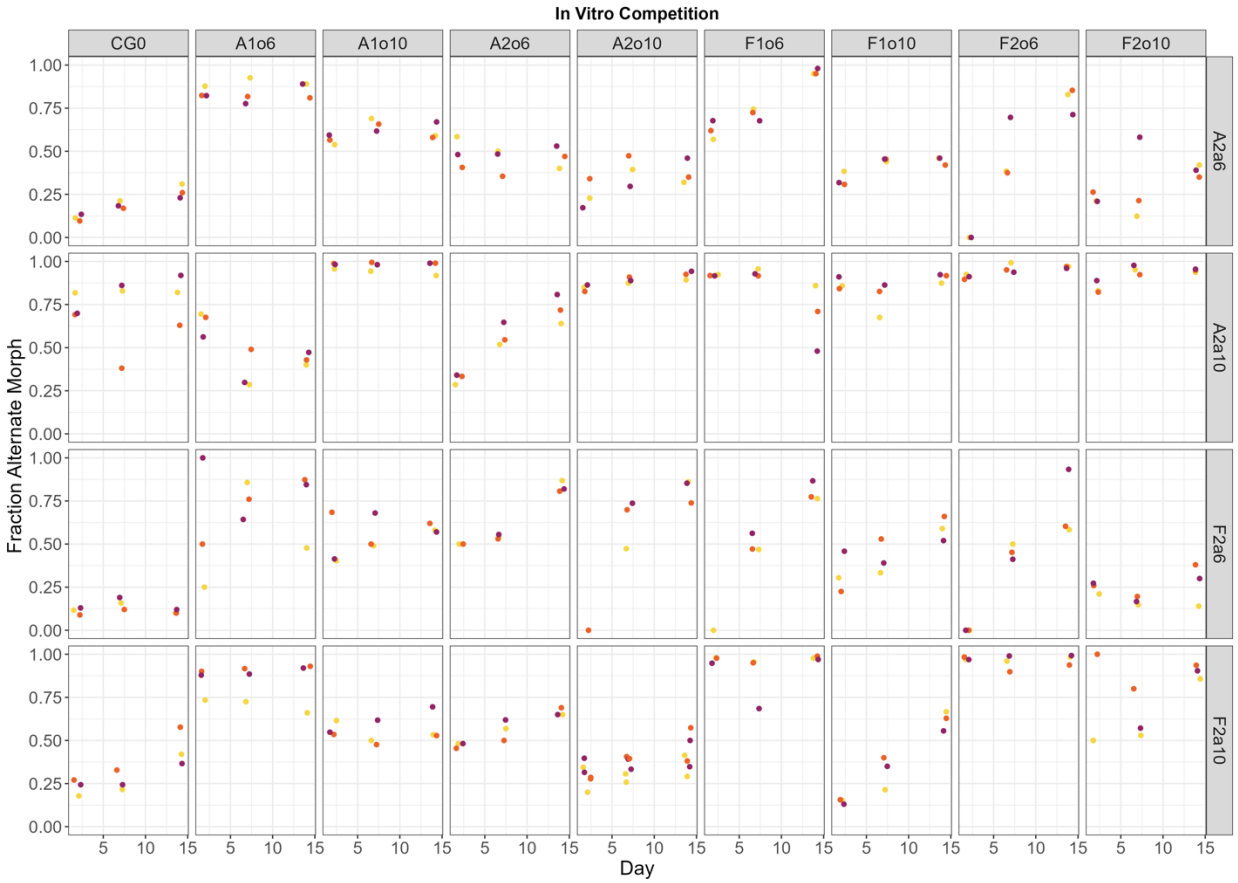

Figure 8. Alternate morphs of *Chryseobacterium gleum* persist *in vitro* on 1.5% NGM agar plates in co-culture with original morphs. Plates were handled identically to those in experimental evolution (Methods). Populations were similar at the end of the first (day 7) and second (day 14) passages for most combinations, and extending a subset of conditions to include one additional passage had no further effect on ratios or abundances (not shown), suggesting that a local ecological equilibrium had been reached for most pairs. Coexistence was observed in all pairs, regardless of whether the original morph was taken from the same passage (6 or 10) as the alternate morph and whether the original morph was from a replicate where alternate morphs did (A2, F2) or did not (A1, F1) exist at passage 10. Ancestral *C. gleum* (CG 0) is used as a reference. Each replicate represents one isolate from the alternate morphology (n=3); the same number of isolates of the original morph within each community and passage were grown individually and pooled to create a common competitor. (Data by Megan Taylor and Marissa Duckett)

As we observed variation in growth between individual isolates and across isolates from different communities and passages, we sought to determine whether these differences could explain the variability in fraction of the alternate morph supported during pairwise competition. We hypothesized that greater growth rate and/or carrying capacity might allow competitive dominance. We therefore plotted differences in growth rate (r_{Alt}-r_{Ori}) and differences in

saturation $\log_{10}$(CFU/mL) in NGM medium (K_{Alt}-K_{Ori}) against the final fraction of alternate morph in pairwise competitions (f_{Alt}) for all pairs of isolates to identify any trends in those data. We observed (Figure 9) that there was no correlation between either exponential growth rate or carrying capacity in liquid NGM and competitive performance in pairwise combinations (Figure 9). Neither of these traits were sufficient to explain the outcomes of inter-specific competition.

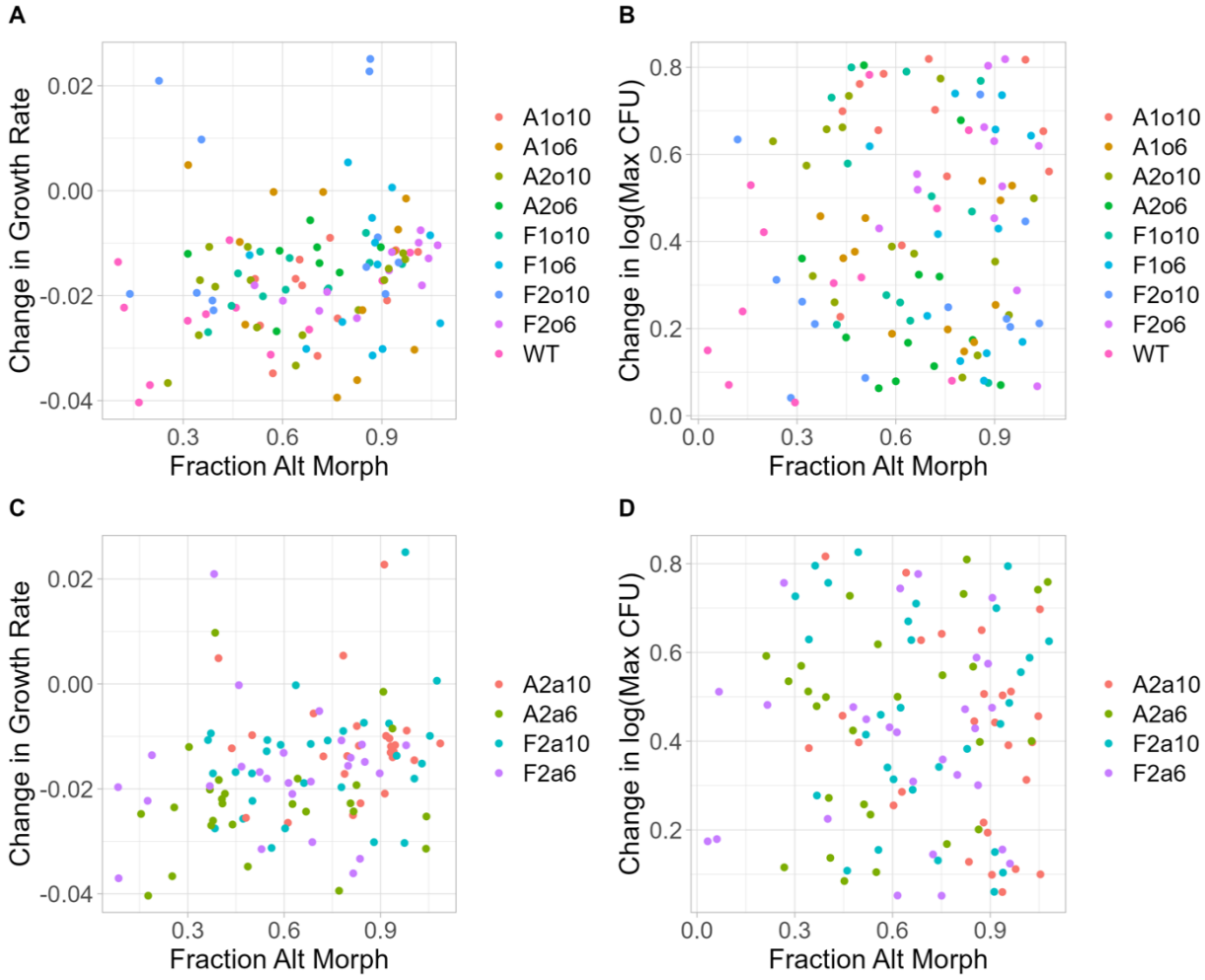

Figure 9. Neither growth rate nor carrying capacity in NGM explain outcomes of pairwise competition. Neither Δr (A, C) nor Δlog(CFU/mL) (B, D) between alternate and original morphs were significantly associated with fraction alternate morph in pairwise competition (linear regression, slopes $p>0.05$). Data are colored by original morph (A, B) and by alternate morph (C, D) to illustrate lack of dependence of these results on community and passage. (Data by Megan Taylor and Marissa Duckett)

Alternate morphs are less motile than original morphs

Previous work has suggested motility as a target for selection (van Ditmarsch et al. 2013). *C. gleum* canonically lacks flagellar motility (Steinberg and Burd 2015). However, several studies have suggested that this clade is capable of gliding motility on the surface of soft (0.35%) agar plates, a trait shared with other members of the *Flavobacteriales* (Sato et al. 2021). Surface motility assays were therefore conducted on soft (0.35%), swarming (0.5%), and solid (1.5%) agar to investigate variations in motility associated with isolates of original and alternate morphs from different communities and passages. We observed surface motility in both alternate and original morphs (Figure 10). As described previously for *Chryseobacterium* (Khare, Chandwadkar, and Acharya 2022), spreading colonies were surface iridescent (Figure 11). Motility increased as agar concentration decreased, and colonies were confined to the agar surface, consistent with gliding motility. This observation was consistent across community, passage, and morph. Alternate morphs were consistently less motile than original morphologies, regardless of community ID and passage number (Wilcoxon rank sum tests on 0.35% agar pass 6 p=1.16e-05, pass 10 4.24e-07; 0.5% agar pass 6 p=2.24e-14, pass 10 p=1.07e-4; 1.5% agar pass 6 p=0.0044, pass 10 p=0.011). Some original morphs appeared to be more motile than the ancestral wild-type; however, variability in these data were high, and small differences cannot be supported with confidence.

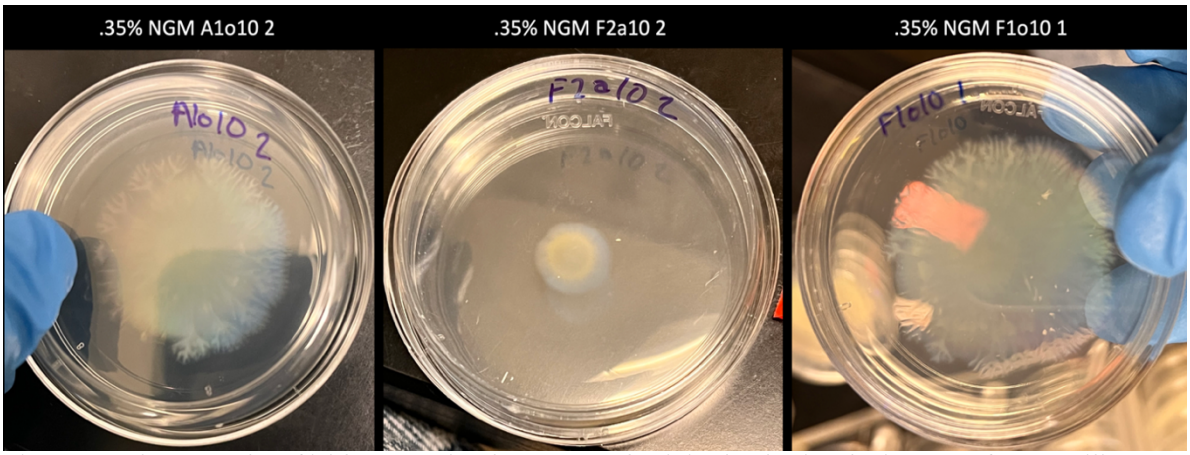

Figure 11. Photographs of iridescence in alternate and original colonies during a surface motility assay on .35% agar NGM plates after 48hrs of growth.

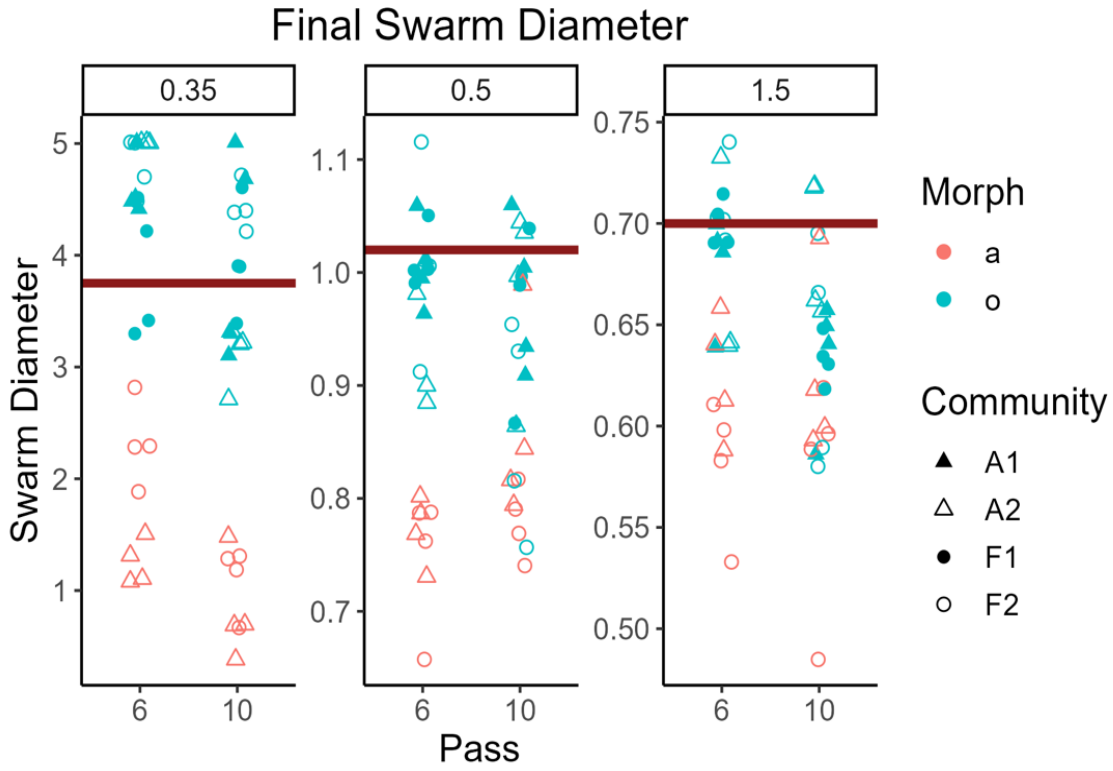

Figure 10. Surface motility of original and alternate morphs of *C. gleum* on 0.35%, 0.5% and 1.5% NGM agar. Diameter of motility in cm is the vertical axis and passage (6 or 10) is the horizontal axis. The red line represents the median diameter of ancestral colonies on the indicated concentration of agar. Blue points are original morphs, red points are alternate morphs; each shape represents one community and replicate (n=4 isolates from single colony picks for each combination of community, replicate, and passage).

There is no observable trend in motility of original morphotypes during adaptation

From initial motility assays, it appeared that motility decreased over passages 6-10. We therefore sought to determine whether there was evidence for directional selection on *C. gleum* motility in these communities. To assess trends in motility over the course of adaptation, isolates of the original morphotype were selected from passages 1-10 of communities A and F, and motility was assessed on soft 0.35% agar; the ancestral strain was used as a baseline. If we observed an increase in motility, this would be an indicator of hypermotility being a developed asset selected for in each community. If we observed a decrease in motility as evolution progressed, this would help explain the rationale for the development and maintenance of less motile alternate morphs. We did not observe any trend in motility over evolutionary time in these isolates, nor did we observe consistent differences in motility between original morphs and the ancestral wild-type (Figure 12). These data do not indicate directional selection on motility.

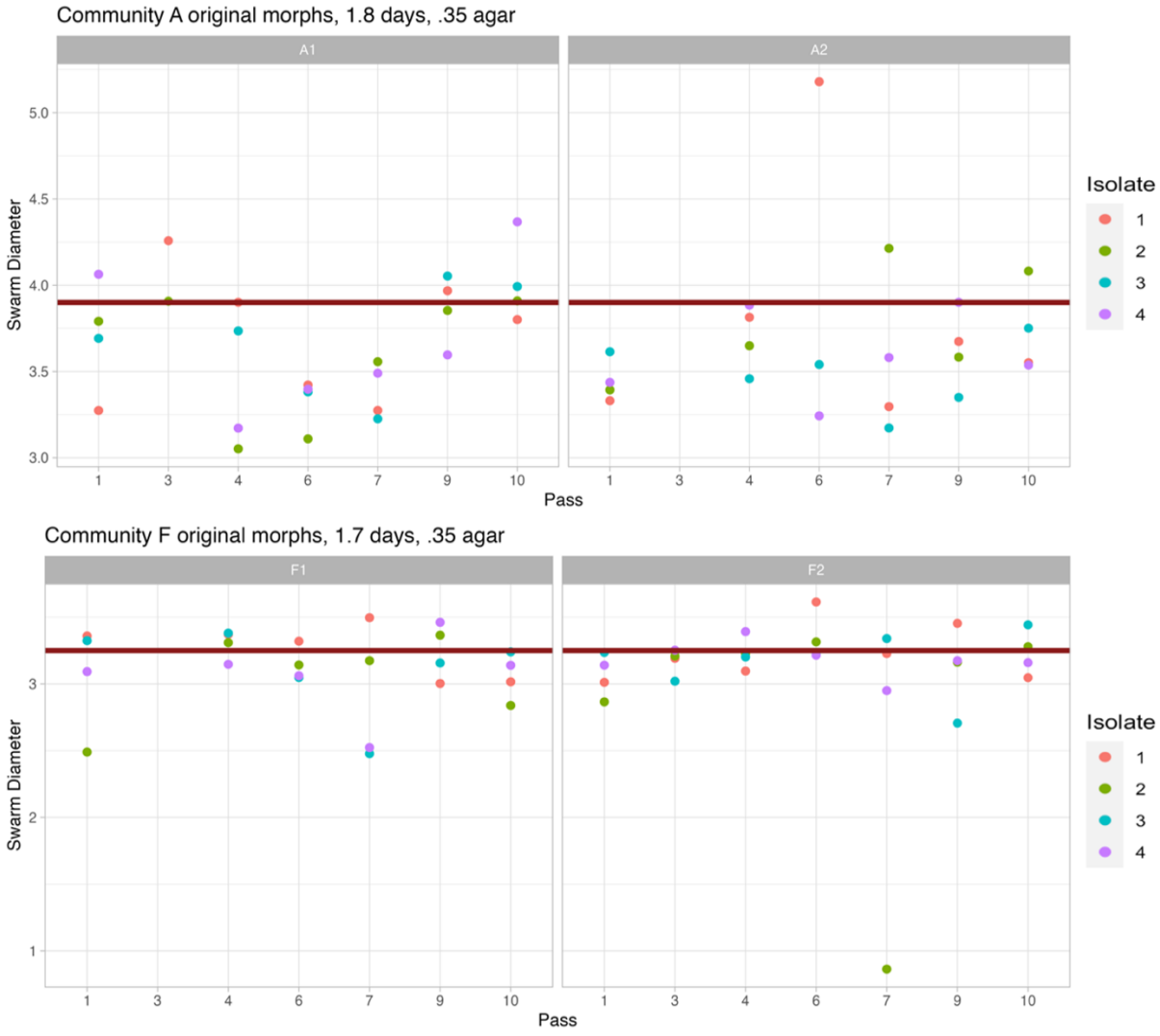

Figure 12. Surface motility of original morphs from passages 1-10 of communities A and F. Isolates from passes 6 and 10 are the same as in the previous figure; all other isolates were retrieved by streaking out glycerol stocks of worm-associated community samples and re-streaking single colony isolates to confirm morphology (n=4 isolates per community and passage). No isolates were available for passage 2 because no samples were frozen during this passage; glycerol stocks of all pass-8 communities, and of community F1 and A2 in pass 3, did not produce colonies. Note that community-A and community-F isolates were assayed on separate days, with separate batches of agar plates, and the raw diameters cannot be compared across runs due to inherent variability in these assays.

Genomic analysis reveals no variability in gliding genes

We next sought to identify genetic differences that would provide insight into causes of changed motility. We hypothesized that a noticeable mutation would be present in motility genes that differentiated alternate and original morphotypes. Eleven strains (A1010, A206, A2a6, A2010, A2a10, WT/Ancestor, F1010, F206, F2a6, F2010, F2a10) were sequenced to identify genomic changes during selection. Overall, we observed very little genetic divergence between isolates (Figure 13).

We sought to identify mutations that might explain observed differences in motility. The genetic basis of gliding in *Chryseobacterium* and other Flavobacteriales is known (McBride and Zhu 2013). Gliding motility in this clade depends on a type 9 secretion system (T9SS) and canonically involves secretion of adhesins (Figure 14). It was hypothesized that genomic variation in the identified gliding motility operon would explain the development of alternate morphologies. All sequenced strains had complete sets of homologs to previously identified components of gliding motility (Figure 14), with the exception that no specific adhesin genes, like SprB, were identified. As compared with the ancestral genome, no SNPs were observed in motility or secretion genes or in regulatory regions associated with any of these genes. The lack of genetic differences between original and alternate morphologies in motility encoding regions indicates that differences in motility between morphotypes did not arise from simple loss or alteration of motility components.

In *Flavobacterium*, motility on firmer (0.5-1%%) agar is dependent on the adhesin SprB (Shrivastava et al. 2013), (Sato et al. 2021), while motility on softer 0.35% agar can occur independently of SprB (Sato et al. 2021). Our original and ancestor morphs displayed easy spreading on soft agar and minimal spreading on agar >0.5%, while the alternate morphs showed reduced spreading ability compared to original morphs at all agar concentrations. Based on these observations, motility in our strains is similar to that of *F. johnsoniae* lacking the SprB

adhesin. Genomic analysis confirmed the absence of SprB homologs or other adhesins in all isolates, and a BLAST search against *Chryseobacterium* revealed no hits for the *F. johnsoniae* operon *sprCDB* (GenBank EF111026.1), indicating the general absence of SprB adhesin in the genus.

SprB-independent gliding using lipoproteins has been observed in Flavobacteriales. In the previous studies on *Flavobacteria*, an initial growth-dependent spreading phase was observed, followed by a period of SprB-independent gliding motility. Mutants lacking various components of the T9SS or gliding genes did not exhibit this secondary expansion phase, underscoring the necessity of gliding for colony expansion. Furthermore, double knockouts lacking both SprB and specific lipoproteins lost motility entirely, indicating the requirement of lipoproteins for SprB-independent colony expansion. The annotated genomes of *C. gleum* do contain the LolA outer membrane lipoprotein, which can facilitate spreading of *Flavobacteria* on soft agar in the absence of adhesin activity (Sato et al. 2021). Notably, we did not observe any SNPs in the *lolA* sequence or adjacent regions, consistent with the lack of mutations in other motility-associated genes.

One possible alternative explanation for motility differences between morphotypes is a change in regulation of motility, for example through mutation of transcription factor(s). In many of our sequenced strains, we see SNPs in Crp- and LexA-family transcriptional regulators. Other SNPs were observed in genes encoding proteins with helix-turn-helix (HTH) domains and IS110 family transposases. At a glance, Crp can regulate transcription by making a Crp-cAMP complex (Soberón-Chávez et al. 2017), LexA acts as a transcriptional repressor in regulation of DNA repair in the SOS regulatory netweork (Simmons et al. 2008), and HTH transcription factors bind DNA and regulate transcription (Menon and Lawrence 2013). IS110 is a transposase that catalyzes transposon movement to another part of the cell (Siguier, Gourbeyre, and Chandler 2014). We do not know what these transcriptional regulators regulate in *Chryseobacterium*

since very little of the genome is annotated, but upstream regulation of factors that affect motility is possible.

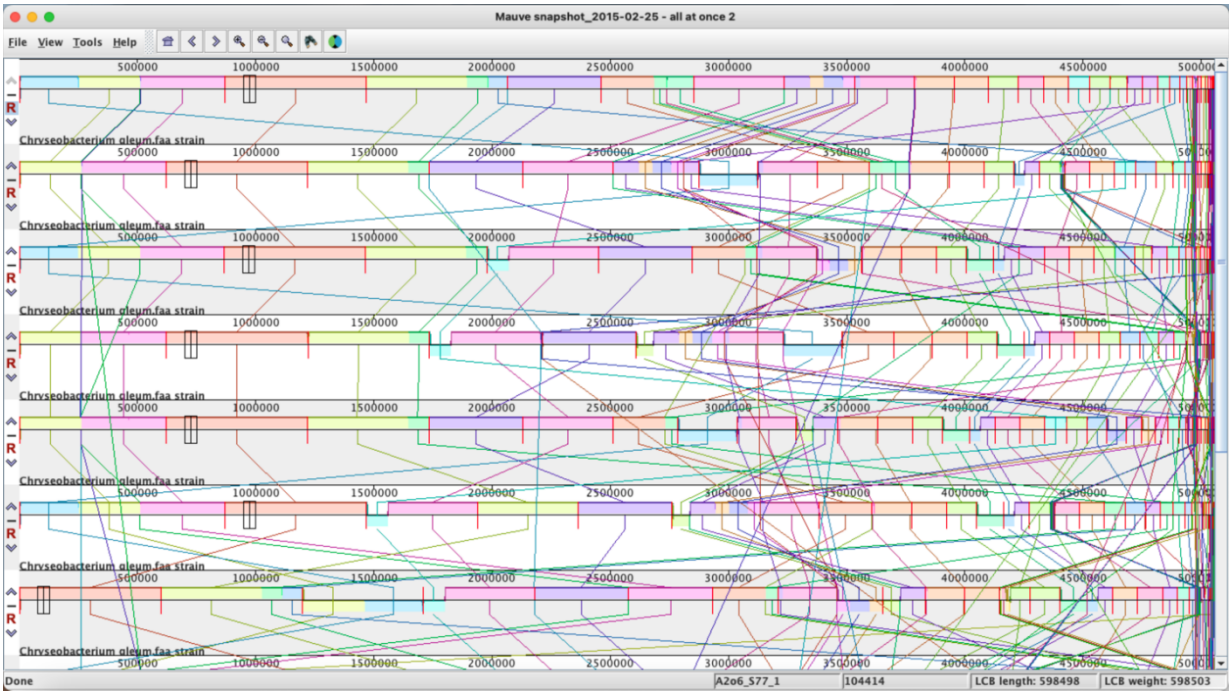

Figure 13. Whole-genome alignment on Mauve. Seven of the eleven sequenced strains are displayed.

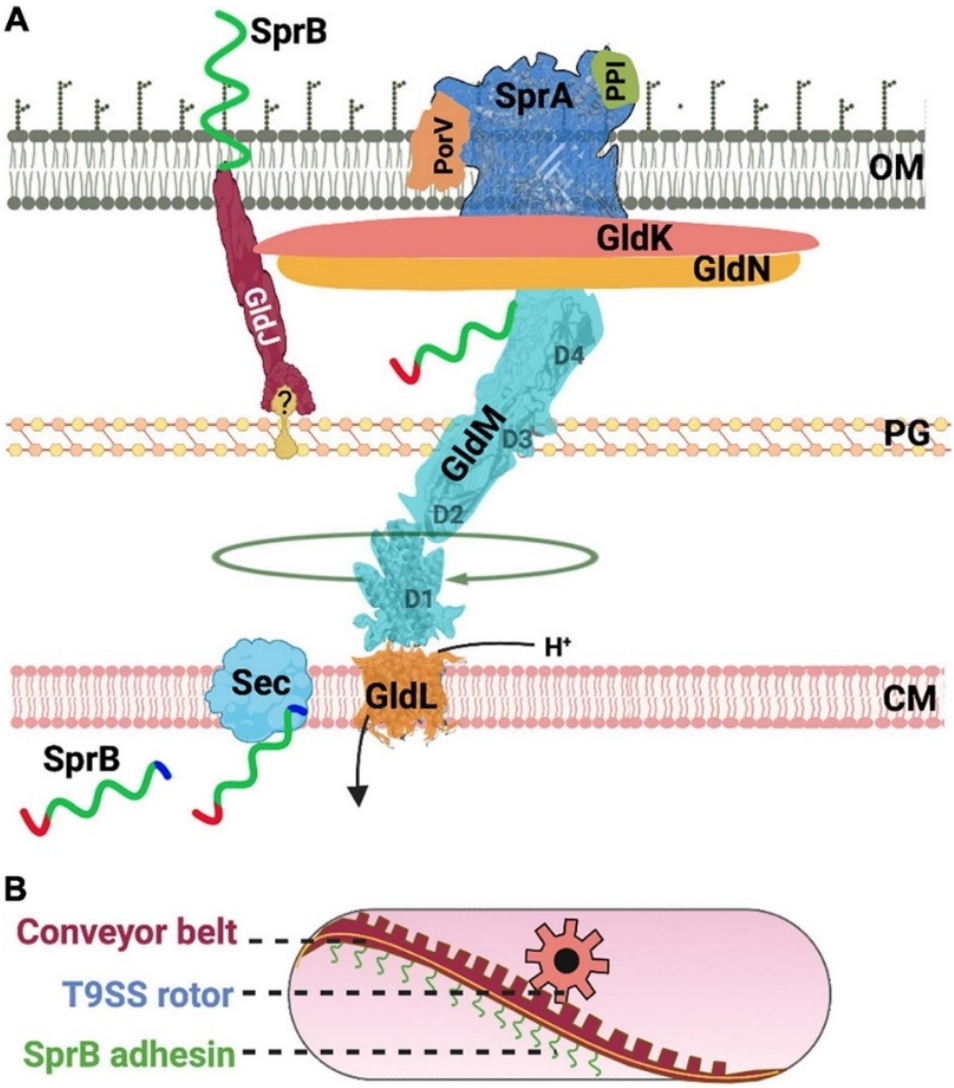

Figure 14. Gliding motility in Flavobacteriales is a function of the Type 9 Secretion System (T9SS). Figure originally published as Figure 2 of (Trivedi et al. 2022), based on the T9SS of *F. johnsoniae* and *P. gingivalis*. The ancestral CG isolate and all other sequenced isolates lack an annotated SprB homolog; in fact, no specific adhesins are annotated on these genomes. These *C. gleum* genomes do show homologs for SprA, PorV, PorP, PorT and all *gld* genes. *gldN, gldM, gldL,* and *gldK* are adjacent to one another and appear to be a single operon; the same is true for *porV, porU*, and *gldJ,* and for *gldB* and *gldC*. **(A)** A cartoon of the nuts and bolts of the T9SS motor that drives protein secretion and gliding motility. T9SS substrates (SprB shown as an example) are transported to the periplasm *via* the Sec transport pathway. The CTD of T9SS substrates is cleaved during transport. A recent model suggests that the proton channel GldL powers the rotation of T9SS. **(B)** A cartoon of the molecular rack and pinion machinery that drives gliding motility. A model based on recent data suggests that the rotary T9SS pinion drives a cell-surface conveyor belt (rack). Cell-surface adhesins such as SprB are secreted by T9SS and are loaded onto the conveyor belt. Interaction of SprB with an external substratum results in screw-like gliding motility of the bacterial cell.

Regulation of motility by nutrient concentration

To explore regulation of motility, we examined motility in varying nutrient densities. Recent studies in a related *Chryseobacterium* (Khare, Chandwadkar, and Acharya 2022) and in *Flavobacterium* (Penttinen, Hoikkala, and Sundberg 2018), (Gavriilidou et al. 2020) indicated that bacteria in this clade alter motility in response to concentration of a rich nutrient source in the media. Higher media concentrations (Difco LB or Shieh medium) resulted in less spread and a smoother frontier, which the authors theorized was due to increased cell density restricting dendritic spread. The 1X NGM medium used in our experiments had a peptone concentration of 2.5 g/L, while the Difco LB medium used in a prior study contained 10 g/L tryptone; 4X NGM is equivalent to 1X Difco LB in tryptone-equivalent concentration, and increased motility was observed over 0.5X-0.02X LB (2X-0.08X NGM).

We hypothesized that nutrient concentration would impact motility based on these observations in previous research. To test this, we assessed motility on 0.35% NGM agar where nutrient concentration was altered by changing the concentration of peptone (0.2X, 1X or 4X standard). In both morphs, growth rate and carrying capacity increased with nutrient concentration in liquid media. Across all conditions, original morphologies were more motile than alternate morphs.

Original and alternate morphs responded differently to the change in nutrient concentration (Figure 15 A). Original morphs showed the most spread on 1X peptone, which was the condition used during experimental evolution. Original morphs expanded almost linearly and to the greatest diameter in 1X peptone, whereas in 0.2X and 4X peptone, the expansion rate and amount of spread was consistently lower. This suggests 1X peptone as the optimal agar for spread of original morphs, inconsistent with previous work on nutrient availability and motility in other Flavobacteriales. Alternate morphs showed linear expansion across the two lower nutrient levels, but at 4X peptone, a lag period was observed.

These trends can be seen more clearly in expansion rates over time (Figure 15 B). For original morphs, expansion is initially rapid and declines over time, except in 1X peptone where expansion is nearly constant over this interval. These trends were not observed in alternate morphs, where rate of spread appears to be constant in all nutrient concentrations, except for an increase over time in 4X peptone conditions.

Neither exponential growth rate (Figure 16) nor carrying capacity (Figure 17) in liquid NGM with different concentrations of peptone were sufficient to explain these results. Maximum spread rate within each morph is about the same across all three nutrient concentrations, but in liquid culture, we see growth rate increasing with nutrient concentration (Figure 16). Saturation density increases with nutrient concentration, but only in alternate morphs is there any correlation with diameter (Figure 17). Further, original and alternate morphs show indistinguishable growth rates at 0.2X and 4X peptone and indistinguishable carrying capacities at 0.2X peptone, but the original morph is more motile across conditions, indicating that the motility differences between morphs are not simply due to differences in growth.

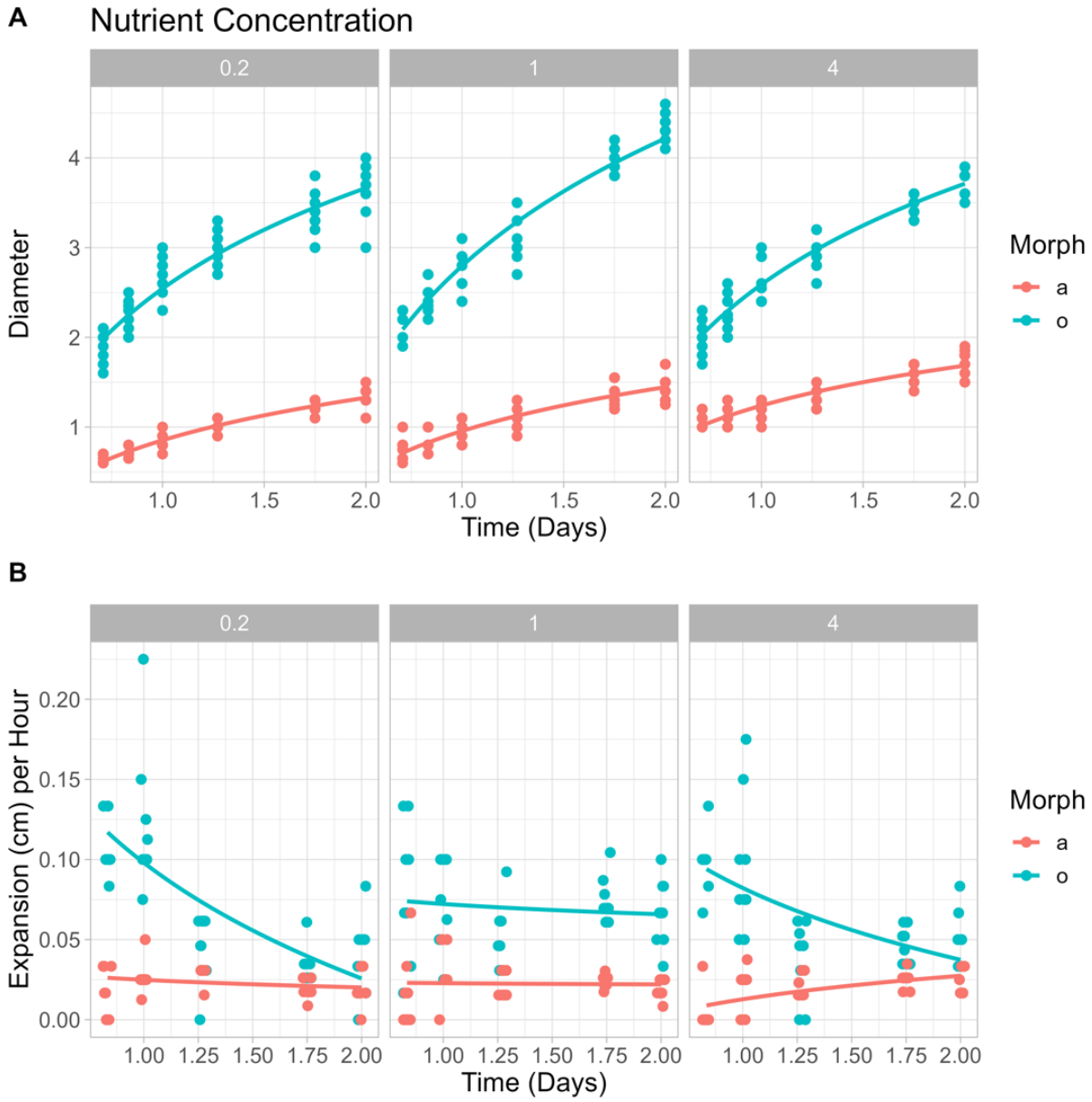

Figure 15. Nutrient concentration alters surface motility on NGM agar. Here, nutrient concentration was altered by changing the concentration of peptone in NGM agar (0.25X, 1X or 4X standard) while holding all other components constant. Strains in these experiments were alternate and original morph isolates from community F2 pass 6 (n=3 isolates per morph, all in technical triplicate; all data points shown). (A) Diameter (in cm) over time. (B) Expansion rates (cm/h) calculated from the data in (A). Lines show log-linear fits to data (y~ln(x)).

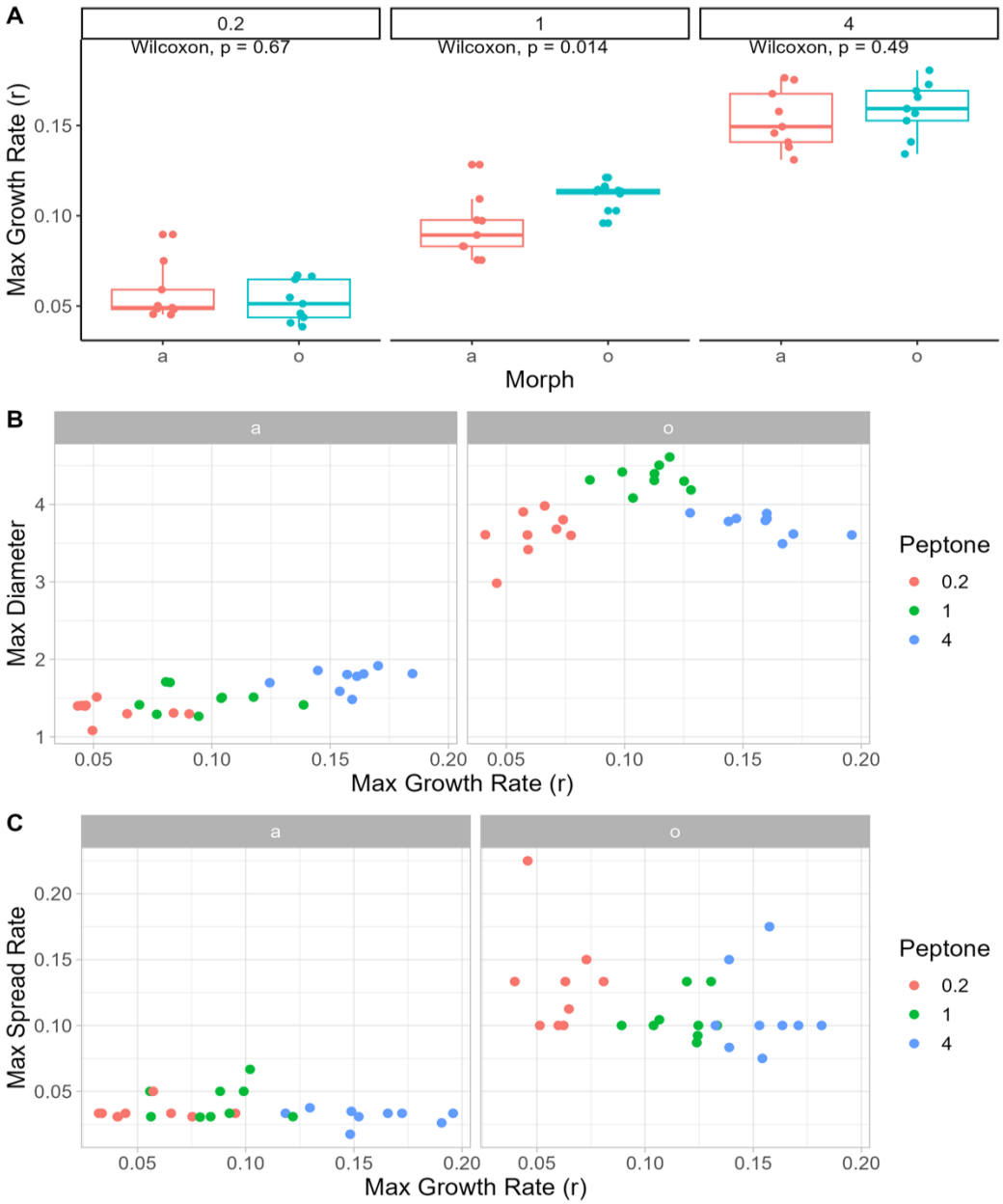

Figure 16. Nutrient concentration alters growth rates, but growth rate does not explain most differences in surface motility. Strains used in these experiments were alternate and original morph isolates from community F2 pass 6 (n=3 isolates per morph, all in technical triplicate; all data points shown). (A) Logistic growth rates were inferred from spline fits to OD600 data when isolates were grown for 24 hours in liquid NGM with 0.25X, 1X or 4X peptone. (B) Logistic growth rates vs maximum diameter (48h growth) on 0.35% NGM plates at each concentration of peptone. For alternate morphs, max diameter and saturation OD are positively correlated (linear slope = 3.7, p=8.8e-06); for original morphs, there is no statistically significant linear correlation (p=0.4). (C) Logistic growth rate vs maximum surface spreading rate on 0.35% NGM agar at each concentration of peptone. Maximum spreading rate and saturation OD are not significantly linearly correlated for either morph (both p~0.25).

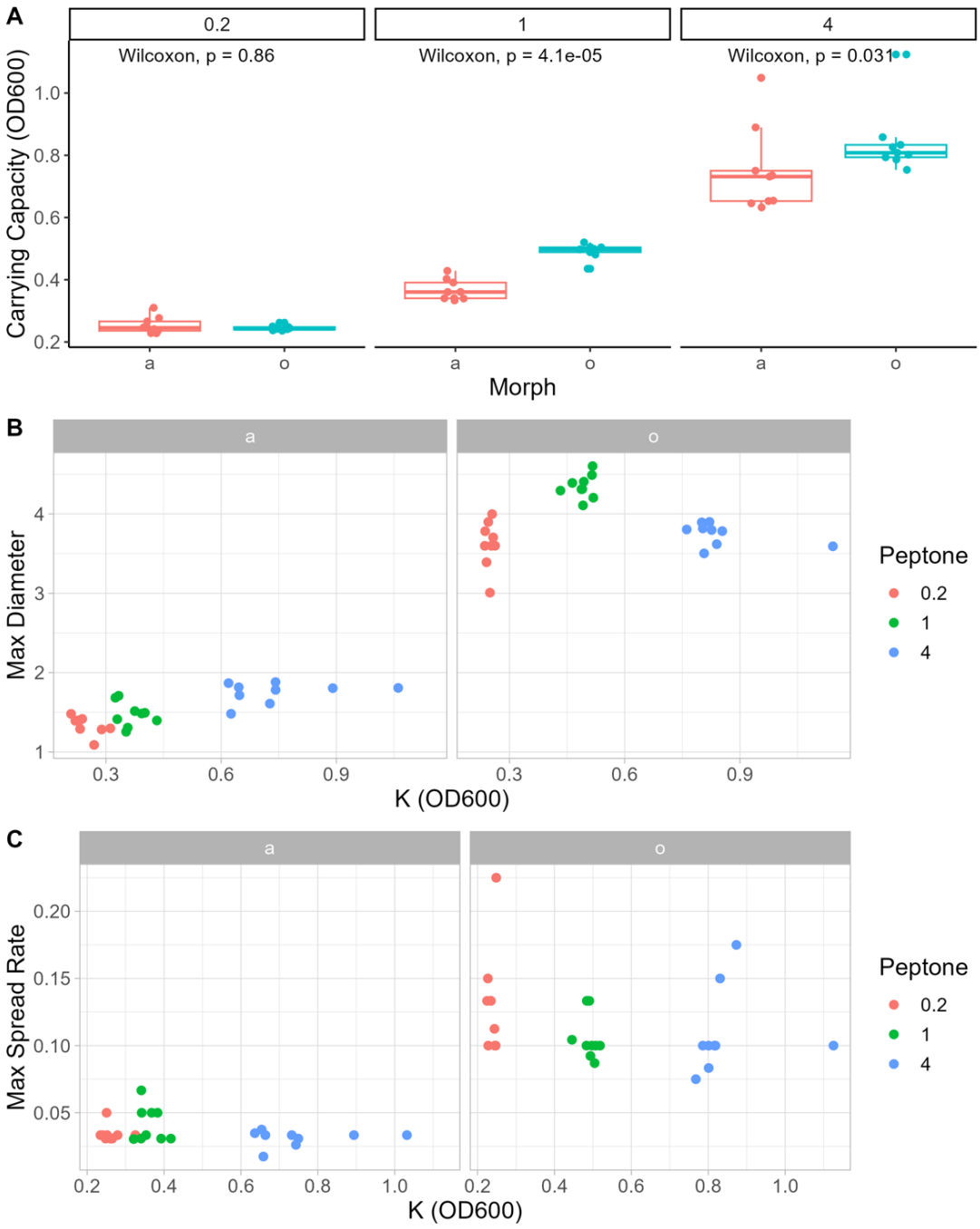

Figure 17. Nutrient concentration alters bacterial density at saturation, but saturation density does not explain most differences in surface motility. Strains used in these experiments were alternate and original morph isolates from community F2 pass 6 (n=3 isolates per morph, all in technical triplicate). (A) Carrying capacities were inferred from logistic model fits to OD600 data when isolates were grown for 24 hours in liquid NGM with 0.2X, 1X or 4X peptone. (B) K vs maximum diameter (48h growth) on 0.35% NGM plates at each concentration of peptone. For alternate morphs, max diameter and saturation OD are positively correlated (linear slope = 0.71, p=4.11e-06); for original morphs, there is no statistically significant linear correlation (p=0.8). (C) K vs maximum surface spreading rate on 0.35% NGM agar at each concentration of peptone. Maximum spreading rate and saturation OD are not significantly linearly correlated for either morph (both p~0.2).

Morphology of the colony frontier, and particularly the branching pattern, were altered by peptone concentration (Figure 18). Both original and alternate morphs produced dendritic spreading colonies on soft agar plates. However, whereas prior work in a different soil-isolated *Chryseobacterium* (Khare, Chandwadkar, and Acharya 2022) observed increased dendritic branching of the expansion front in lower concentrations of peptone, in both alternate and original morphs, the lowest nutrient condition (0.2X peptone) showed nearly smooth edges. In our original morphs these branches are thickest and most pronounced at the intermediate peptone concentration (1X NGM) and are smaller and less pronounced in the lowest and highest peptone concentrations (.2X, 4X). In alternate morphs, by contrast, we see more defined dendritic frontiers as peptone concentration increases. This is consistent with the hypothesis that the differences in motility between original and alternate morphs are due to differences in regulation of the phenotype.

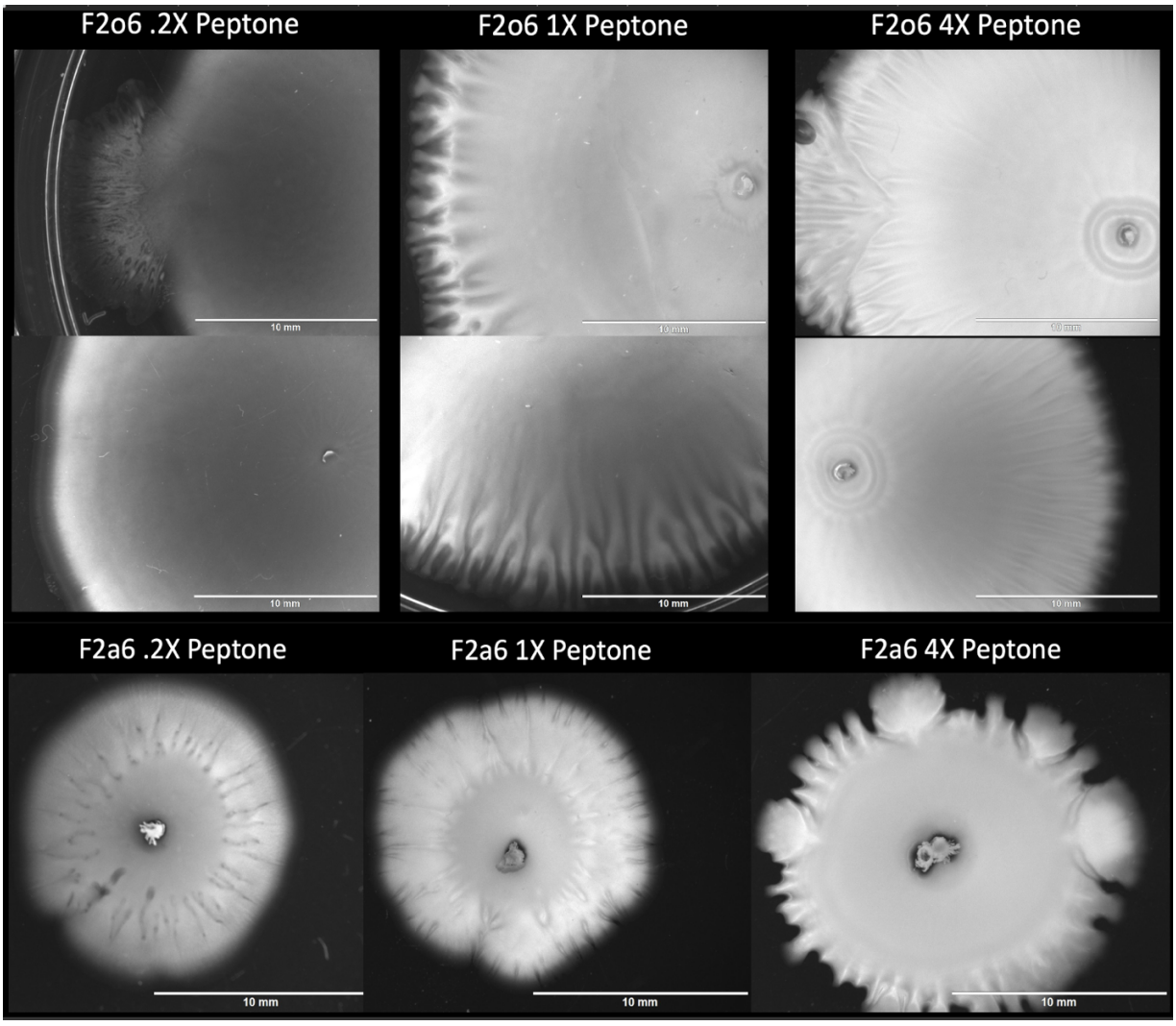

Figure 18. Dark-field microscopy of colony frontiers on 0.35% NGM agar at 48 hours growth.

Discussion

The full scope of variability of species in host-associated and host-independent communities is not understood, and we also don't know what selective pressures cause the emergence of this variability. To investigate these gaps in knowledge specifically in host-associated communities, we characterized host-associated communities based on phenotype to reveal variation and potential selective pressures. Our study reveals convergence in community composition over time, but the development of alternate and original morphologies indicates evolutionary

variability within microbial lineages. The emergence of morphological variation within microbial communities is driven by unidentified selective forces that impact the evolutionary trajectory of individual species. *C. gleum* emerged as a dominant member of the bacterial community despite its limitations as a mono-colonizer. This observation suggests the existence of environmental or inter-bacterial selective pressures that contribute to the increased prevalence of *C. gleum* in community settings. Our research unravels some of the possible selective pressures responsible for within-species variation.

C. gleum emerged as the dominant species in host-associated communities where it was initially present, despite consistently being driven extinct on plates without the worm and despite performing poorly as a mono-colonizer of the worm (Taylor, Janasky, and Vega 2022). In previous work with this system (Taylor, Janasky, and Vega 2022), mono-colonization ability did not predict performance of bacteria in communities, and specifically there was no trend with mono-colonization ability and community composition in *C. gleum*. Further, *C. gleum* is a pathogen, causing substantial death in adult N2 worms within one day of exposure (Figure 5); in fact, colonization by these bacteria is difficult to measure due to worm loss. Despite high relative abundance in communities, *C. gleum* populations measured from worm digests during these experiments were numerically small, generally <1000 bacteria per worm. This suggests that *C. gleum* populations in the worm intestine were small and short-term, and the environmental space is likely where *C. gleum* is best maintained. The fact that *C. gleum* performs poorly when mono-colonizing worms, but can rise in prominence when it is part of a greater microbial community, suggests that selection for within-host performance is unlikely. The selective pressures acting on *C. gleum* in these experiments are not at present clear.

We did observe some changes in growth parameters, including differences in growth parameters between original and alternate morphs. Growth rate and carrying capacity are often causes of competitive advantages and can give perspective of the type of selection in an environment.

Alternate morphs show lower exponential growth rates than the ancestor, while original morph growth rates are largely indistinguishable from the ancestor. Since *C. gleum* is prey in this host-microbe system, it could reasonably be hypothesized that growth rate would increase, but this was not observed. Alternately, to evade predation, microorganisms can become more difficult to consume. *C. elegans* shows behavioral avoidance of very thick lawns (Demir et al. 2020). Alternate morphs, and many of the pass-10 original morphs, have a greater carrying capacity than ancestor. It is plausible that increased colony density evolved to evade consumption by the host. Since this increase in carrying capacity is in both alternate and original morphs, we cannot conclude that carrying capacity is a source of differentiation of the morphs.

All isolates of *C. gleum* displayed surface motility, which encompasses gliding, swarming, twitching, and sliding, which are the fastest forms of bacterial motility (Verstraeten et al. 2008), (Palma et al. 2022). In the Bacteroidota phylum, flagella and swimming/swarming motility are absent, and motility is primarily achieved through T9SS-dependent gliding (Paillat et al. 2023). We confirmed that the *C. gleum* isolates were capable of surface movement on soft agar, indicating the utilization of gliding motility. Moreover, the essential genetic components of gliding motility were conserved across all tested isolates without any observed mutations. This aligns with previous findings in other Flavobacteriales, where altered morphologies associated with reduced motility were not linked to mutations in motility-associated genes (Penttinen, Hoikkala, and Sundberg 2018).

Motility has been previously identified as a target of selection *in vitro* and in host-associated bacteria. In a prior run of this experiment, we observed differences in swimming motility in an invading *Pseudomonas mosselii* isolated from different communities. Isolates from community I2 passage 9 were observed to be hypermotile, while the remainder communities and passages from the experiment reflected ancestor-like motility. This demonstrates variation in motility within species and between communities. This difference in motility from different starting

communities indicate a variation in motility as evolution occurs as a result of unknown selective pressures. In another experiment, with host-independent non-communal *Pseudomonas aeruginosa,* swimming motility was observed to increase during experimental evolution (van Ditmarsch et al. 2013). This trend towards hypermotility was not observed in our experiments. Directional selection on motility during experimental evolution was not observed. However, we do observe less motile morphotypes that emerge after six passages, highlighting that experimental evolution somehow contributes to the selection and maintenance of less motile morphotypes in *Chryseobacterium gleum*.

To explore regulation of motility, we examined motility in varying nutrient densities. Our results were inconsistent with recent studies in a related *Chryseobacterium* (Khare, Chandwadkar, and Acharya 2022) and in *Flavobacterium* (Penttinen, Hoikkala, and Sundberg 2018) which indicated that bacteria in this clade increase motility in response to decreased concentration of a rich nutrient source in the media. This suggests variation in motility regulation within *Chryseobacterium*.

These previous studies used complex rich media (LB and Shieh medium) that contained yeast extract, while our study employed nematode growth medium (NGM) containing peptone but without yeast extract. Although it is clear that motility in Bacteroidota is influenced by the environment, the specific impact of this difference on motility in Bacteroidota remains uncertain. Furthermore, it is unknown whether the response to nutrient concentration differs across communities or replicates, and whether evolved original-morph isolates display different motility responses compared to the ancestral wild type. Future investigations will compare motility among these isolates in different media types to address these questions.

In our surface motility and nutrient assays, we observed distinct expansion patterns between alternate and original morphs. Original morphs displayed rapid spreading across a range of nutrient concentrations, resulting in similar final spread diameters despite visually different cell

densities in the expanding colonies. This suggests these morphs are capable of density-independent gliding motility, as observed in *sprB* deficient *Flavobacterium* (Sato et al. 2021). Understanding the spreading of alternate morphs is more challenging, as their expansion, growth rate, and carrying capacity all increased with nutrient concentration. To further explore density dependent and independent spread, surface motility assays can be conducted with inocula of different concentrations for original morphs. This would allow us to speculate on a threshold for density dependent spread, and to see if original morphs are capable of density independent spread.

Changes in regulation can often be associated with tradeoffs within an organism. Change in motility is usually the result of a regulatory change (Ottemann and Miller 1997). Frequently, mutants in lineages of motile biofilm-forming bacteria show a tradeoff between these two phenotypes, which can lead to morphological and phenotypic variation within a clade (Palma et al. 2022), (van Ditmarsch et al. 2013). In *Flavobacterium johnsoniae*, removal of individual gliding motility genes and T9SS genes inhibited both biofilm formation and motility, indicating that the genes used for gliding motility are also required for biofilm formation (Eckroat, Greguske, and Hunnicutt 2021). With this known overlap in motility and biofilm formation machinery, it is reasonable to expect that there is a relationship between nutrient concentration and regulation of motility and biofilm in *Chryseobacteria* as well.

We do not have data on biofilm formation in our isolates. Based on prior work in related bacteria, we presume that these *C. gleum* are capable of biofilm formation, and it is reasonable to assume that the T9SS is important for both motility and biofilm formation in these isolates as in other Bacteroidota (Penttinen, Hoikkala, and Sundberg 2018). It is possible that reduced motility in alternate morphs might be linked to enhanced biofilm formation. Future work will compare motility and biofilm formation among these isolates in different media concentrations to address this question.

We also want to understand what contributes to the synchronous emergence of alternate morphologies in different communities. *C. gleum* morphological variants arose in different communities at the same time, pass 6, and were maintained for the duration of the experiment, pass 10. This emergence coincides with the loss of community biodiversity, so this change in community context may be somehow associated with the emergence of within-species diversity. This could be tested in community-based competition assays to determine whether alternate morphs can be sustained in different biodiverse conditions. Two comparative communities could be ancestor-rich and ancestor-poor. The ancestor-rich community would include all seven original ancestral isolates, and ancestor-poor communities would contain only species remaining in these communities as of pass 6. For both communities, *C. gleum* alternate morphs would be added to starting conditions. This assay would confirm whether alternate morphs can arise in biodiverse conditions, or if their emergence is a consequence of reduced community biodiversity.

While broader community dynamics tend to foster convergence, it is crucial to acknowledge that individual microbial species exhibit distinct evolutionary trajectories within these communities. Investigations encompassing both within species, community, and passage-level dynamics and within-species variation are pivotal in unraveling the complex nature of microbial community evolution.

Methods

Strains and culture conditions. Bacterial strains in Table 1 were obtained from the USDA Agricultural Research Service (ARS) Culture Collection (NRRL). Strains showed characteristic morphology on salt-free nutrient agar (NA, 3g yeast extract, 5g peptone, 15 g agar per L), which was used for identification of colonies (Taylor, Janasky, and Vega 2022). Combinatorial communities were set up with mixtures of seven strains as shown in Table 2**.**

N2 Bristol *C. elegans* were provided by the *Caenorhabditis* Genetics Center, which is funded by NIH Office of Research Infrastructure Programs (P40 OD010440). Stocks of ancestral N2 worms were cultivated on 10 cm NGM agar plates at 25°C with *E. coli* OP50 as a food source according to standard protocols (Stiernagle 2006).

Species	Abbreviation
B-2879 *Arthrobacter aurescens*	AA
B-1876 *Bacillus spp.*	BS
B-14798 *Chryseobacterium gleum*	CG
B-14848 *Chryseobacterium indologenes*	CI
B-24236 *Microbacterium oxidans*	MO
ATTC 49188 *Ochrobactrum anthropi*	OA
B-1574 *Rhodococcus erythropolis* (mucoid)	RE15M
B-1574 *Rhodococcus erythropolis* (dry)	RE15D
B-16025 *Rhodococcus erythropolis*	RE16
B-23393 *Sphingobacterium spiritivorum*	SS
B-14902 *Sphingobacterium thalpopium*	ST

Table 1. These species are the eleven *C. elegans*-naïve soil bacterial isolates selected from USDA NRRL soil bacteria collection used to create communities. Three of seven genera (*Chryseobacterium, Rhodococcus, and Sphingobacterium)* are represented by more than one species or isolate.

Bacteria: AA, MO,BS, OA, RE15D, RE15M, RE16, CI, CG, SS, ST							
Multispecies Combinations							
A	AA	MO	RE15D	BS	OA	CG	SS
B	AA	MO	RE15D	BS	OA	CG	ST
C	AA	MO	RE15D	BS	OA	CI	SS
D	AA	MO	RE15D	BS	OA	CI	ST
E	AA	MO	RE15M	BS	OA	CG	SS
F	AA	MO	RE15M	BS	OA	CG	ST
G	AA	MO	RE15M	BS	OA	CI	SS
H	AA	MO	RE15M	BS	OA	CI	ST
I	AA	MO	RE16	BS	OA	CG	SS
J	AA	MO	RE16	BS	OA	CG	ST
K	AA	MO	RE16	BS	OA	CI	SS
L	AA	MO	RE16	BS	OA	CI	ST

Table 2. Combinatorial composition of each of the twelve seven-species starting communities A-L.

Community-based experimental evolution. Community-based evolution was carried out as in (Taylor, Janasky, and Vega 2022), with minor modifications. To observe the outcomes of community-based host-associated evolution in a simple microbial community, we initiated experimental evolution of combinatorial minimal communities of bacteria (see Tables 1 and 2) with and without the nematode *C. elegans* as predator and host (see Figure 1 for workflow schematic). Worm+ plates were initiated with synchronized L1 larvae of wild-type Bristol N2 *C. elegans*. Larvae were aliquoted in equal volumes (approximately 100 L1 larvae per plate) onto 6 cm NGM agar plates with pre-grown and UV-killed lawns of *E. coli* OP50 + 50 µL total NRRL bacteria at 10^8 CFU/mL. Starting cultures of NRRL bacteria were pre-grown individually in 1 mL LB cultures for 48 hours at 25°C, transferred to 1.5 mL Eppendorf tubes, and centrifuged 2 minutes at 9000xg in a tabletop centrifuge (Eppendorf) to pellet. Supernatant was removed, and bacteria were re-suspended in 1 mL S medium before being diluted to 10^8 CFU/mL in a second

Eppendorf tube with a final volume of 1 mL S medium. These 10^8 CFU/mL stocks were combined in equal ratios to form the communities in Table 2, and these mixtures were used to seed plates. All communities were established in duplicate.

Every 7 days, plates were observed and scored on a 0-4 scale for number of total worms, number of larvae, and plate coverage by bacterial lawn; observations were recorded in summary for each bacterial strain or combination until differences between replicates were observed, at which point scores for each replicate were recorded individually. After scoring, plates were washed once with 1 mL M9 worm buffer + 0.1% Triton X-100 (M9TX01) to remove the bulk of the worms and the bacterial lawn. The resulting suspension was centrifuged briefly in a small benchtop centrifuge to pellet worms, then washed again with 1 mL M9TX01. The second wash was drawn down to 100 µL and supernatant was discarded; worms were re-suspended by flicking, and 10 µL of the worm- and bacteria-containing liquid was transferred to a fresh room-temperature plate of NGM + UV-killed OP50. Motorized pestle batch digests were performed to determine bacterial community composition in the intestines of adult worms according to standard protocols for this lab (digests in 20 µL M9TX01 in 0.5 mL tubes, Kimble Kontes) (Taylor and Vega 2021); target was 50 individual worms, but if this number was not available, all adults in the sample were counted and digested. Samples of live worms and bacterial contents from batch digests were individually frozen. Single colony picks were taken from digest plates (up to 6 isolates per species per replicate), grown in 100 µL LB in 96-well plates for 48 hours at 25°C, then mixed 1:1 with 40% glycerol and covered with aluminum sealing foil before freezing at -80°C.

For community-based evolution in the absence of worms, a slightly modified protocol was used. Plates were initially established with ancestral communities as already described, but on 6 cm NGM plates without UV-killed OP50 as this initial worm food source was not needed. Every 7 days, plates were washed with M9TX01 to remove the entire bacterial lawn, centrifuged for 2

minutes at 6000xg to pellet, and resuspended in 1 mL S medium by pipetting. The resulting suspension was diluted in a ten-fold series for plating and CFU counting, and 10 µL of a 1:10 dilution of each suspension was aliquoted onto the center of a fresh 6 cm NGM plate to seed communities for the next passage. Plates were grown upside down at 25°C. Samples were cryopreserved as already described.

Pairwise bacterial interactions in vitro. To determine whether alternate and original morphs could coexist and to measure competitive ability or morphs within and between replicates and passages, we competed pairs of individual isolates in culture in the absence of the host. The isolates used in these experiments were randomly selected from worm digest plates from each passage, re-streaked on fresh NA plates to confirm morphology, and cryopreserved as single colony picks at -80°C. Isolates of CG from passage 6 and 10 worm+ communities A1, A2, F2, and F2, as well as the ancestral strain (n=3 isolates per morph per condition), were grown up separately in 1 mL LB cultures for 24 hours at 25°C and diluted to a uniform cell density of 10^8 CFU/mL. Isolates of the original morph from each community + passage were combined into a single volume. For pairwise competitions, the indicated pooled original morph was mixed 1:1 with each individual alternate morph isolate. 5 µL of each pairwise competition mix was mixed with 90 µL S medium in a 96 well plate. 10 µL of each well was transferred to the center of two 6 cm NGM plates (1.5% agar, poured fresh, not dried), and plates were moved to 25°C to grow. At indicated time points (2, 7, and 14 days), lawns were washed off plates (see *Community-based experimental evolution*) and resuspended in 1 mL 1xPBS. These resuspensions were serially diluted ten-fold in 1xPBS (200 µL final volume per well) and plated in 100 µL aliquots on 10 cm nutrient agar (NA) plates for CFU counting and identification of original and alternate morphs. On day 7, fresh plates were inoculated with 10 µl of the first (1:10) serial dilution and grown for 7 days for sampling on day 14.

Chryseobacterium gleum Mortality Assays. As we observed host mortality in mono-colonization experiments with these isolates, we sought to determine whether *C. gleum* was pathogenic to *C. elegans*, and whether evolved and ancestral isolates differed in pathogenicity. Isolates of *C. gleum* ancestral strain (ANC) as well as isolates obtained from worm+ community plates in passages 6 and 10 were grown separately in 1 mL LB cultures for 48 hours at 25°C and diluted to a uniform cell density of 10^8 CFU/mL. The isolates used in these experiments are the same randomly-selected isolates as in the previous section. 50 µL of each isolate were plated onto separate 6 cm NGM plates in triplicate. Plates were grown up at 25°C for 48 hours to develop a lawn. Using a BioSorter (250FOCA, Union Biometrica), 50 sucrose washed adult N2 worms were plated onto the resulting lawns. Plates were incubated at 25°C, and worms were scored every 24 hours for four days. Worms that were not moving independently and did not respond to prodding with a worm pick were scored as dead.

Growth curves. To quantify the phenotypic consequences of experimental evolution and assess variation among isolates within these samples, we conducted a series of experiments to assess growth and motility. Bacteria isolated from evolved communities and ancestral isolates for each strain were grown up separately in 1 mL LB cultures for 24 hours at 25°C, then diluted in liquid NGM to a uniform cell density of 10^8 CFU/mL. Each strain was then further diluted 1:100 to a final cell density of 10^6 CFU/mL in 150 µl liquid NGM in a clear polypropylene 96-well plate (3-4 replicates per strain, each from a separate single colony isolate). The plate was covered with BreatheEasy Sealing Membrane and was run on a BioTek Synergy HTX plate reader using a 24-hour kinetic protocol reading OD600 every 10 minutes at 25°C. Growth curve data were analyzed in R using the function *SummarizeGrowthByPlate*() in *growthcurver* to infer carrying capacity of the logistic growth model from the OD600 over time data from each individual well; maximum growth rates were inferred for each well using *many.splines.fit()* from package *growthrates*. Parameter values were calculated for all replicates for each individual strain, and

summary statistics (mean, median, variance) were calculated across experiments for each replicate.

Surface motility. Surface motility was assayed using a canonical drop culture assay. For worm-independent motility, swarm motility assays were conducted with only *Chryseobacterium gleum* on 6 cm NGM agar plates with 0.35%, 0.5%, or 1.5% agar. 6cm plates were filled with 8mL of agar on the day of experiment and allowed to solidify lid-off for 30 minutes in a laminar flow hood to help ensure uniform surface moisture across plates),(. Bacterial cultures were grown overnight in 100 µL of LB in individual wells of a 96-well plate at 25°C, shaking, and covered with USA Scientific BreatheEasy Sealing Membrane. Cultures were transferred 1µl to 100 µl liquid NGM the morning of the experiment and allowed to re-grow under the same growth conditions for 4 hours. 1 µl drops of each NGM culture were carefully placed in the center of each plate, avoiding splatter. Plates were incubated in stacks of not more than three plates at 25°C in the dark, with a tray of water providing ambient humidity. 1.5% and 0.5% plates grew for 7 days. 0.35% plates grew for 2-3 days due to the swarms reaching the edge of the agar plate. Swarm diameter was measured with a ruler using centimeters and millimeters. Measurements were conducted 3-12 hours apart.

In assays to determine the effects of nutrient concentration on motility, the same protocol was followed, with the exception that 0.35% NGM agar was made with peptone at 0.2X (0.5 g/L), 1X (2.5 g/L), or 4X (10 g/L) of the standard formulation. All other components were kept constant according to the standard formulation for NGM agar.

DNA extraction and genome sequencing. Isolates were sent for whole genome sequencing to determine what mutations were produced during adaptation. Cultures were grown individually overnight in 1mL cultures of LB (25°C, shaking). Samples were centrifuged at 13,000 RPM for 2 minutes to pellet cells. Cells were washed with 1 mL 1xPBS three times, resuspended in 1 mL PBS, and separated into 5 PCR tubes (200µl each). To improve lysis efficiency, a freeze-boil

protocol was used: samples were frozen in a -80C freezer for 10 minutes, then immediately boiled in a thermocycler for 10 minutes. This step was repeated once more. After freeze-boil, samples were recombined in 1.5 mL Eppendorf tubes and centrifuged at 13,000 RPM for 2 minutes; supernatant was discarded. DNA extraction was carried out using the Promega Wizard DNA Extraction Kit reagents and protocols, with addition of 10 µL proteinase K (20 mg/mL, MolBio or Invitrogen) and 50 µL lysozyme (20 mg/mL, MolBio) to the lysis step (incubated 30 minutes at 37°C in bead bath to allow lysis to proceed) (Natarajan et al. 2016). Samples were rehydrated with 50µl rehydration solution for 1hr at 65°C.

DNA concentration of each sample was measured with both Qubit and Nanodrop. Qubit measurements were made using protocols and reagents from Invitrogen Qubit High Sensitivity Assay. BioTek Synergy HTX plate reader Nanodrop measurements were conducted using 2µl of sample and 2µl of Promega rehydration Buffer as the blank on a Take3 plate. Samples above 20ng/µl were sent to Microbial Genome Sequencing Center (SeqCenter) for 200Mbp Illumina sequencing with NovaSeq 6000.

Quality control and assembly were performed in Bactopia (Petit and Read 2020) using default parameters, with reference to a species-specific dataset (Ariba reference datasets, RefSeq mash sets, and GenBank sourmash) including full genome assemblies of up to 1000 genomes identified as *C. gleum*. Variant calling was performed against the complete reference genome for each strain sequenced.

Mauve was used to identify SNPs from multiple genome alignment of the reference sequence, each individually-evolved isolate, and the ancestral genome. The alignment with the reference genome was used for identification of SNP-containing loci when possible. When no homolog was available in the reference genome, or when homologs were not annotated with gene names or specific functions, nearest homologs were identified via nucleotide megaBLAST (high

homology) or BLASTn (somewhat dissimilar sequences) against *Chrysobacterium gleum* and *C. cucumeris*.

Data availability. All data and code used in this manuscript are available at https://github.com/veganm/2022NRRL2_AltMorphs

Table of Figures

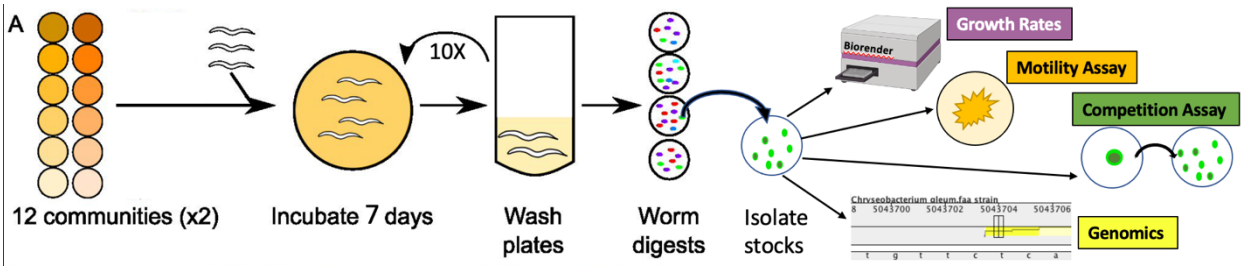

Figure 1 Experimental workflow for community-based evolution. The experimental set up for the previous project consisted of 12 seven member communities, similar at a genus level but variable on a species level. Each community had a replicate made, resulting in A1 and A2 communities and the like. These communities were grown with worms and passaged every seven days to fresh NGM agar plates. Worm digests were conducted to reveal the bacterial community composition. Isolates were picked, this revealed species variability. Isolates reflective of original and alternate morphologies were used in phenotypic variability testing. Growth rates and carrying capacity were measured in a plate reader. Motility assays were conducted on agar plates with variable agar. Competition assays were conducted by growing an alternate and original morph together then plating them, the amount of each morphotype was counted to quantify which was a stronger competitor. Genomics were conducted with specific

strains, SNPS and their corresponding genes were identified. The image displays a SNP on a *C. gleum* genome. 3

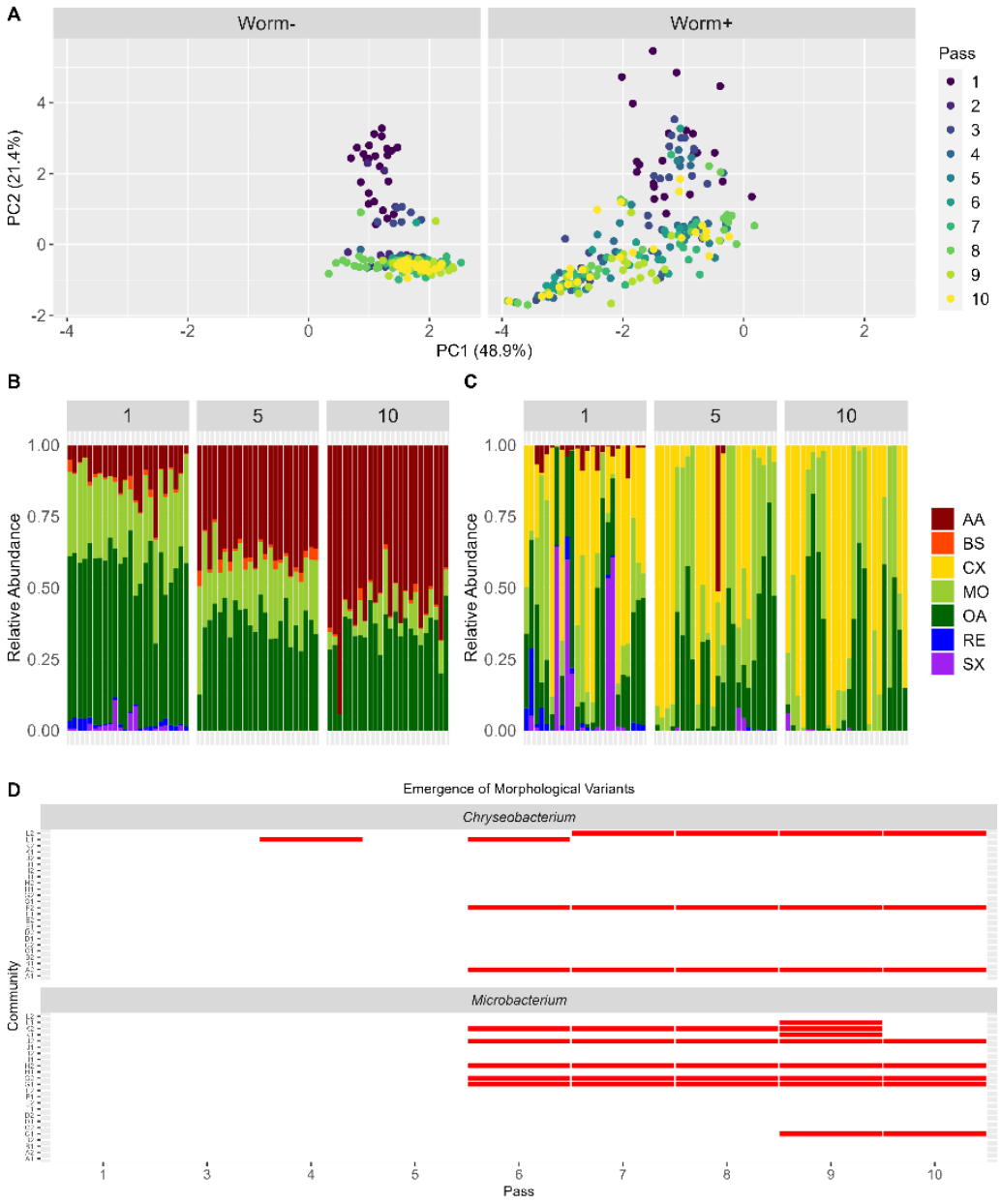

Figure 2 . Community-based adaptation produces convergent community composition along with diversification within and between communities. (A-C) Community composition follows coherent trajectories over time in the presence (right) and absence (left) of C. elegans, with compositional differences associated with the presence of worms. For plates with worms (right),

data are from batch digests of adult worms taken from plates at the end of each passage (n=50 adult worms per batch). For plates established without worms (left), data are for communities washed from plates. (A) PCA of community composition data over time (ten passages of experimental evolution) Each point represents one replicate (12 communities, two replicates each). (B, C) Relative abundance for communities in passages 1, 5, and 10; each bar represents one replicate as in (A). Communities are shown in order of community ID and replicate number (community A replicate 1, A replicate 2, B replicate 1, B replicate 2…; two replicates for each of 12 communities, n=24 bars). Here "CX" refers to either CG or CI, "RE" refers to RE15D, RE15M, or RE16, and "SX" refers to either SS or ST, according to the starting composition of the individual communities (**Table 2**). C. gleum (CG) is the Chryseobacterium isolate in communities A-B, E-F, and I-J (two replicates each: columns 1-4, 9-12, 17-20 out of 24 in panels B-C). (D) Emergence of morphological diversity in worm-associated communities. Community replicates are on the y-axis (in reverse order top to bottom, L2->A1). Passages where two distinct morphotypes were observed for Chryseobacterium (top) and Microbacterium oxydans (bottom) are marked in red. (Data by Megan Taylor)..... 6

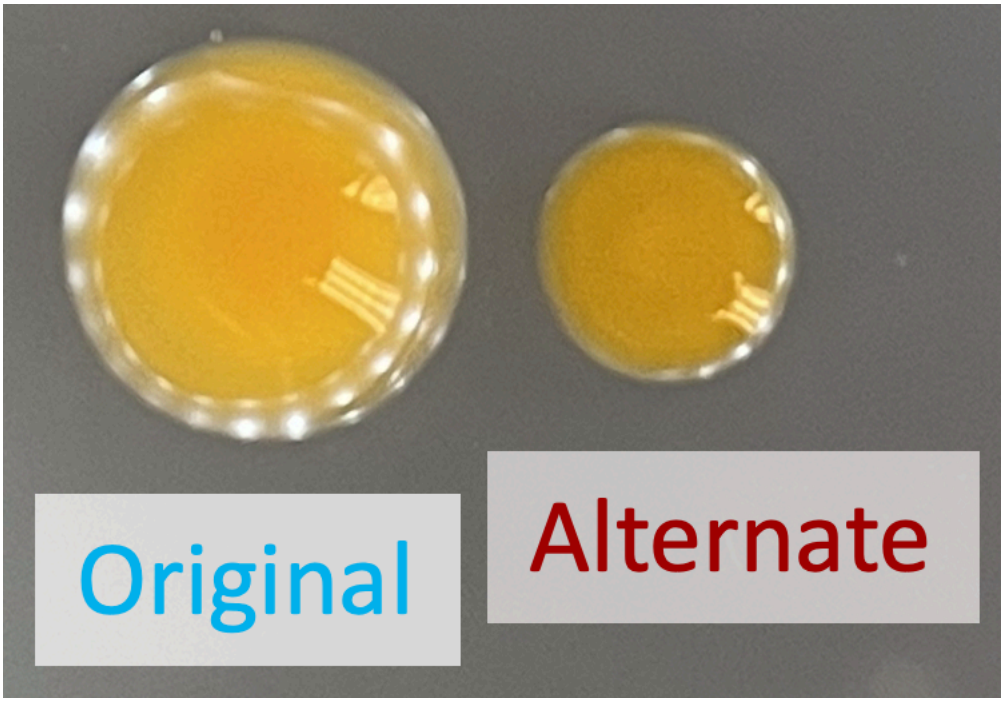

Figure 3. Phenotyping of original (o) and alternate (a) morphs of *C. gleum*, based on distinct phenotypes on salt-free nutrient agar. The original morph is brightly colored, glossy, round, smooth, and slightly mucoid. The alternate morph is smaller and flattened, with less opacity and duller coloration. 7

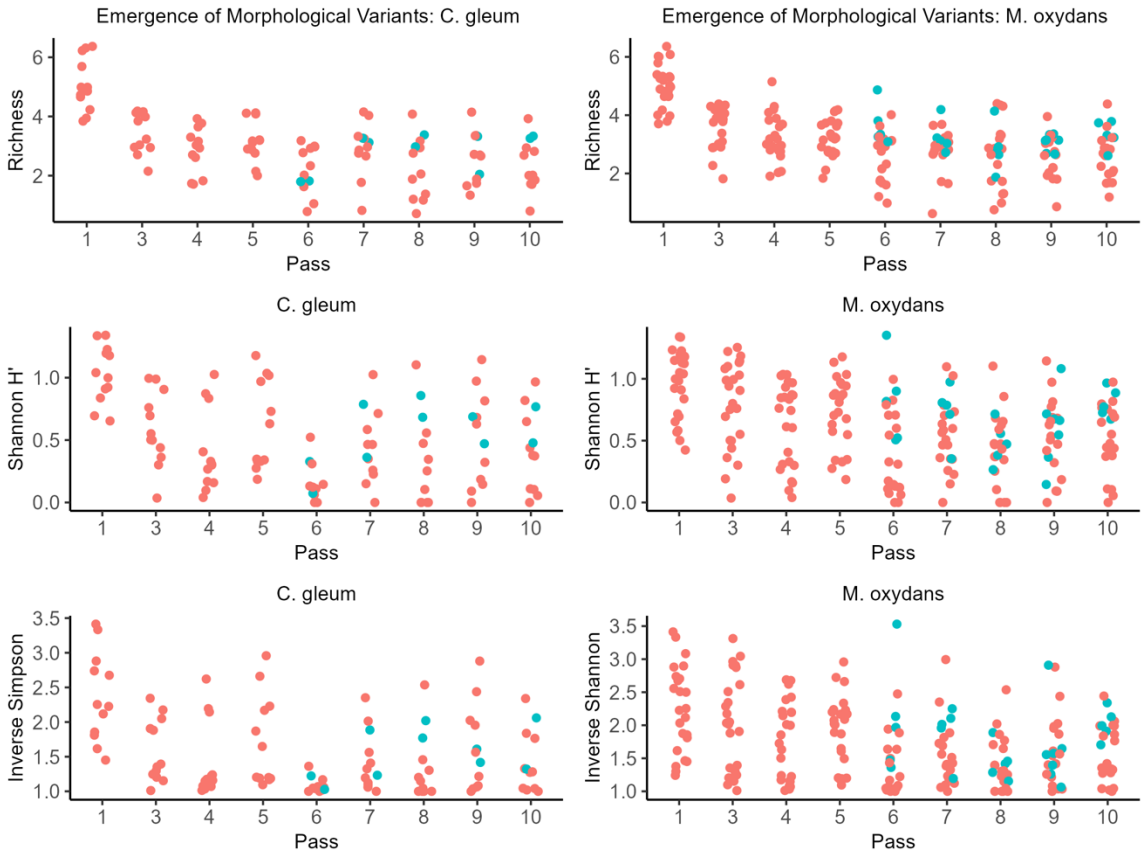

Figure 4. Emergence of alternate morphs of *C. gleum* (left) but not *M. oxydans* (right) coincides with time-series minimums of taxonomic diversity. Each data point represents one of two replicates of each community (n= 12 points for 6 communities containing *C. gleum* and 24 points for 12 communities containing *M. oxydans* at each passage). Communities without alternate morphs are shown in pink; communities with alternate morphs of the indicated species are shown in blue. Each row reports a different measure of community diversity (richness, Shannon H', inverse Simpson). (Data by Megan Taylor).....7

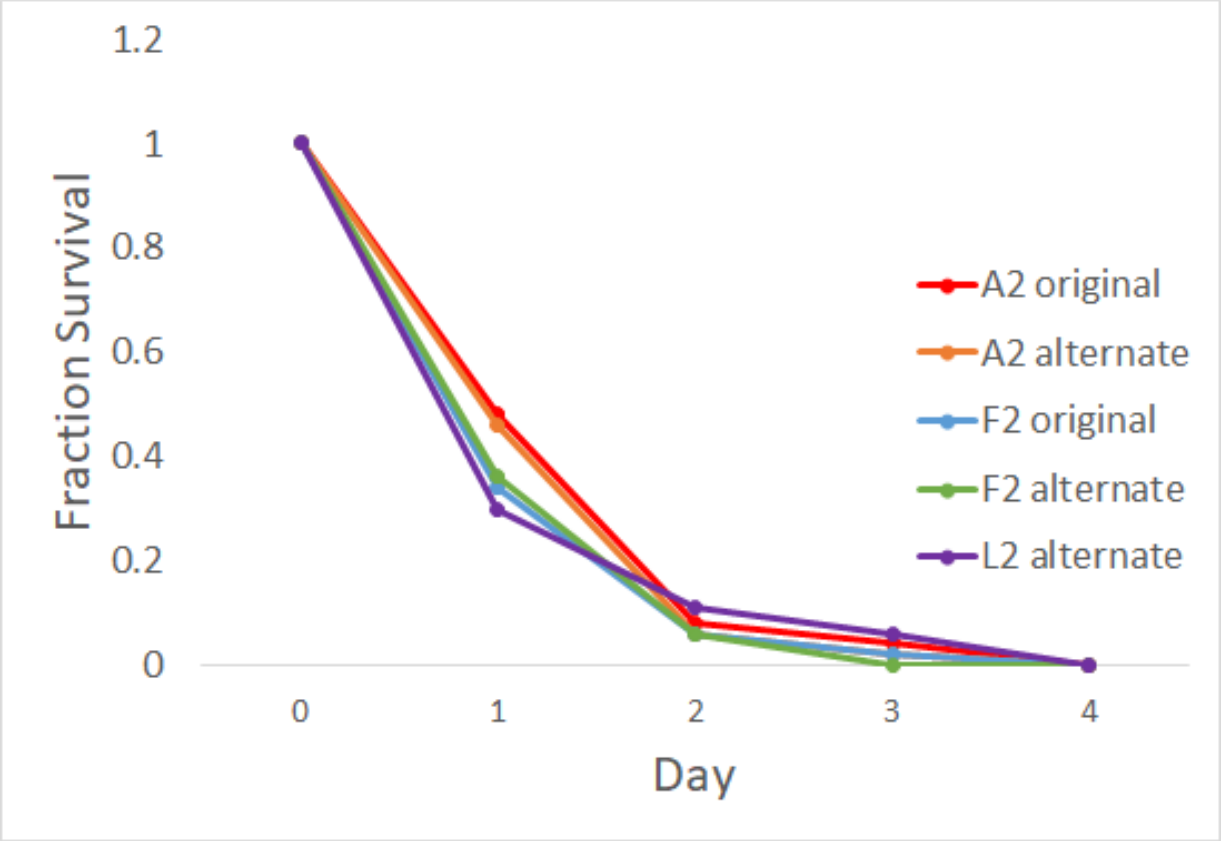

Figure 5. *Chryseobacterium gleum* kills N2 Bristol *C. elegans*. In these assays, day 2 synchronized adult worms (n=100) were added to 6 cm NGM plates with lawns of pass-10 isolates of *C. gleum*. Mortality was assessed at 24 hour intervals. (Data by Megan Taylor) 8

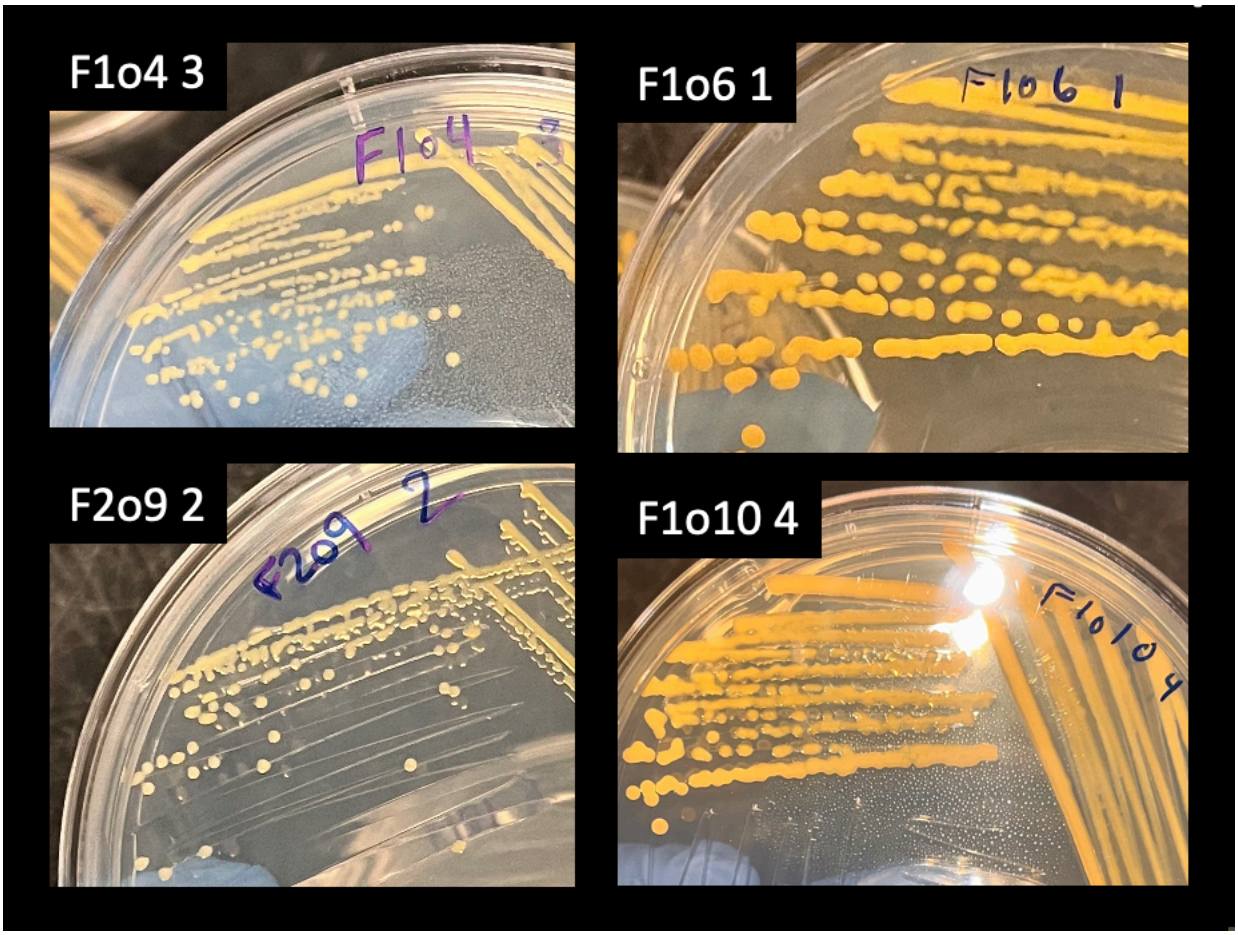

Figure 6. Variation in colony morphology within the “original” morphotype in Community F1, passages 4, 6, 9, and 10. Photos were taken of two-day old nutrient agar plates. 9

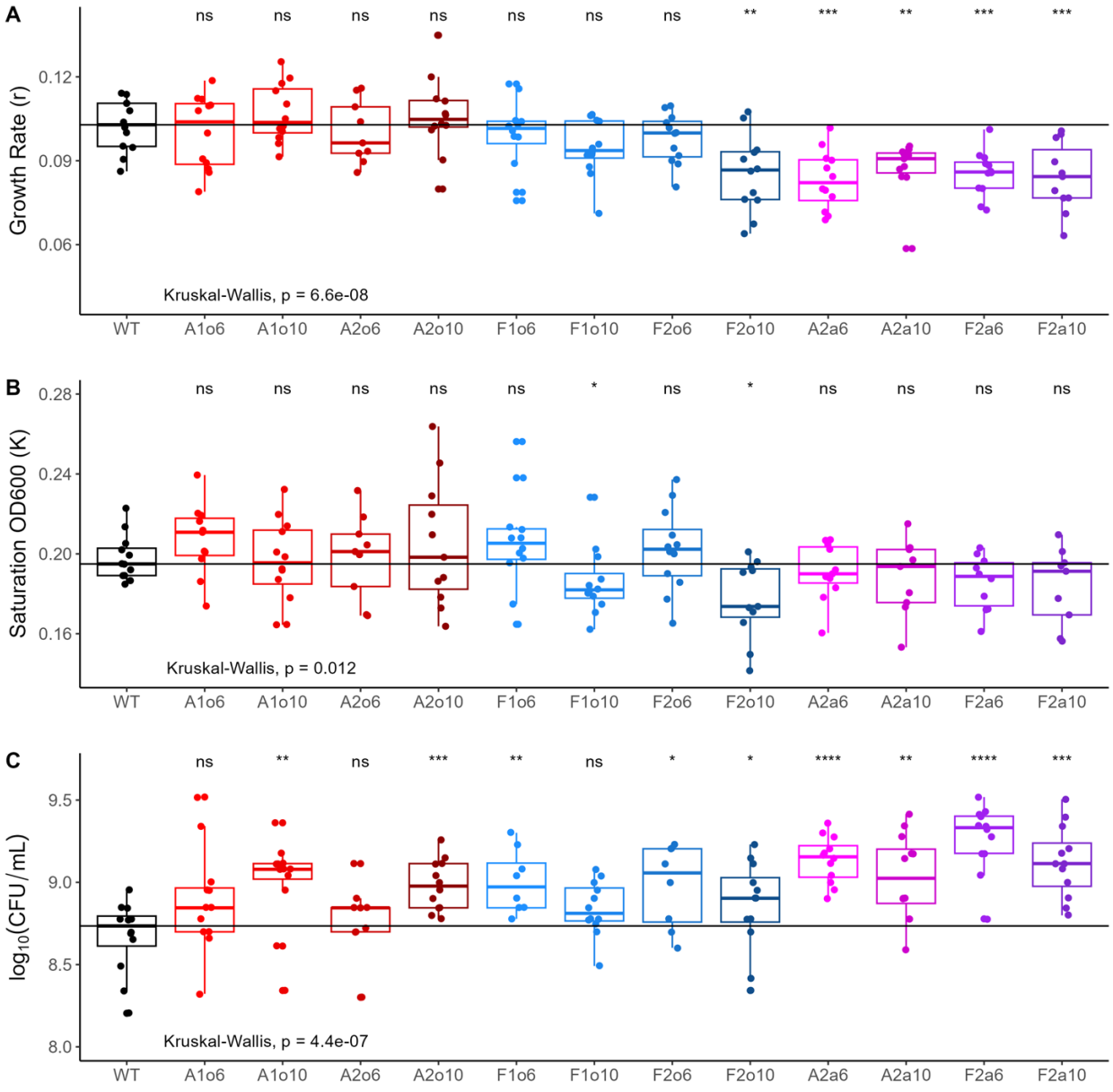

Figure 7. Phenotyping of *C. gleum* original (o) and alternate (a) morphs from communities A and F. Ancestral isolates are shown as "WT". Maximum exponential growth rate (h^{-1}) (A) and OD600 saturation density (B) were estimated from plate reader growth curves in liquid NGM media at 25°C. Saturation density in CFU/mL (C) was estimated by dilution plating the same cultures after 24 hours growth in plate reader. Data represent three independent experiments on separate days, using the same isolates in all runs (n=4 from each community and passage).

Results of pairwise Wilcoxon rank sum tests against the ancestor are shown above each data set (*, p<=0.05; **, p<=0.01; ***, p<=0.001; ****, p<=0.0001). 11

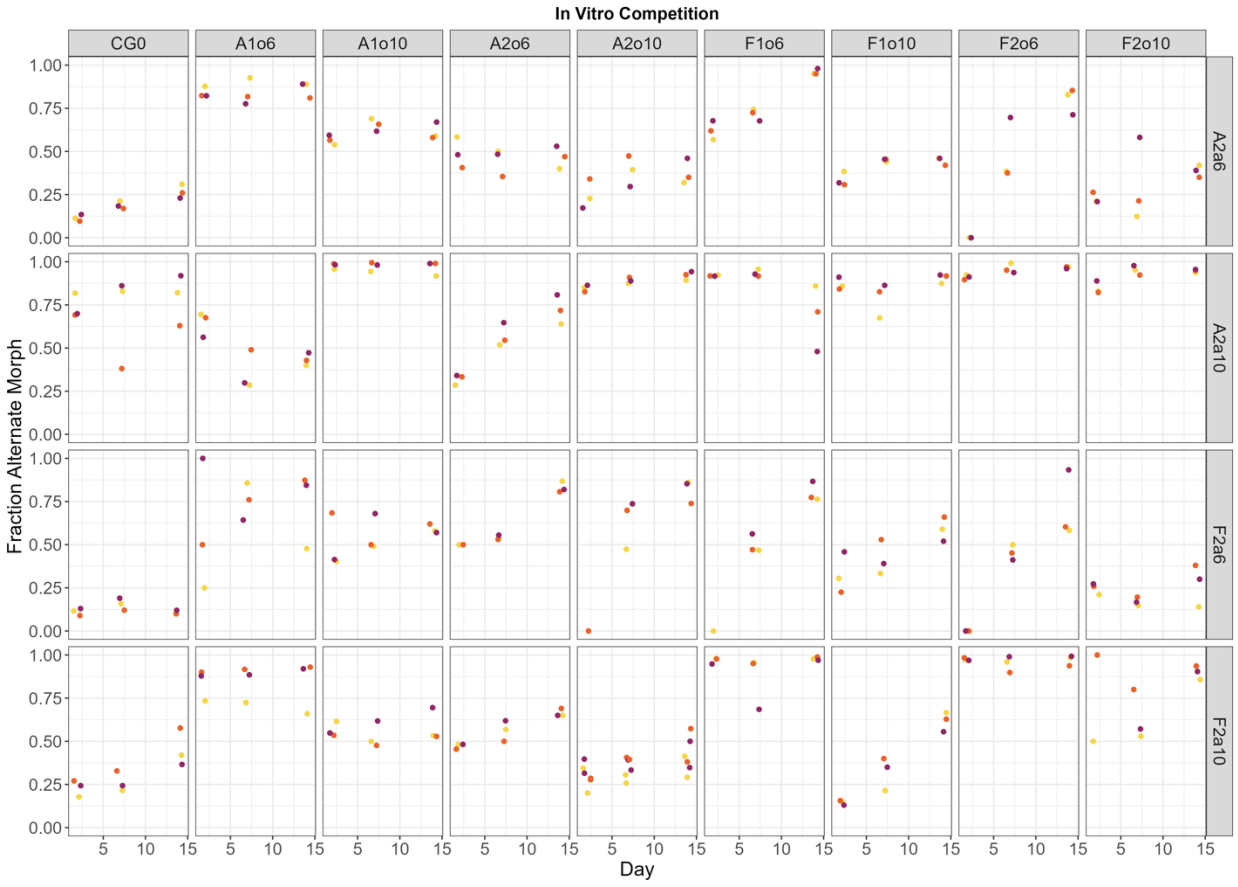

Figure 8. Alternate morphs of *Chryseobacterium gleum* persist *in vitro* on 1.5% NGM agar plates in co-culture with original morphs. Plates were handled identically to those in experimental evolution (Methods). Populations were similar at the end of the first (day 7) and second (day 14) passages for most combinations, and extending a subset of conditions to include one additional passage had no further effect on ratios or abundances (not shown), suggesting that a local ecological equilibrium had been reached for most pairs. Coexistence was observed in all pairs, regardless of whether the original morph was taken from the same passage (6 or 10) as the alternate morph and whether the original morph was from a replicate where alternate morphs did (A2, F2) or did not (A1, F1) exist at passage 10. Ancestral *C. gleum* (CG 0) is used as

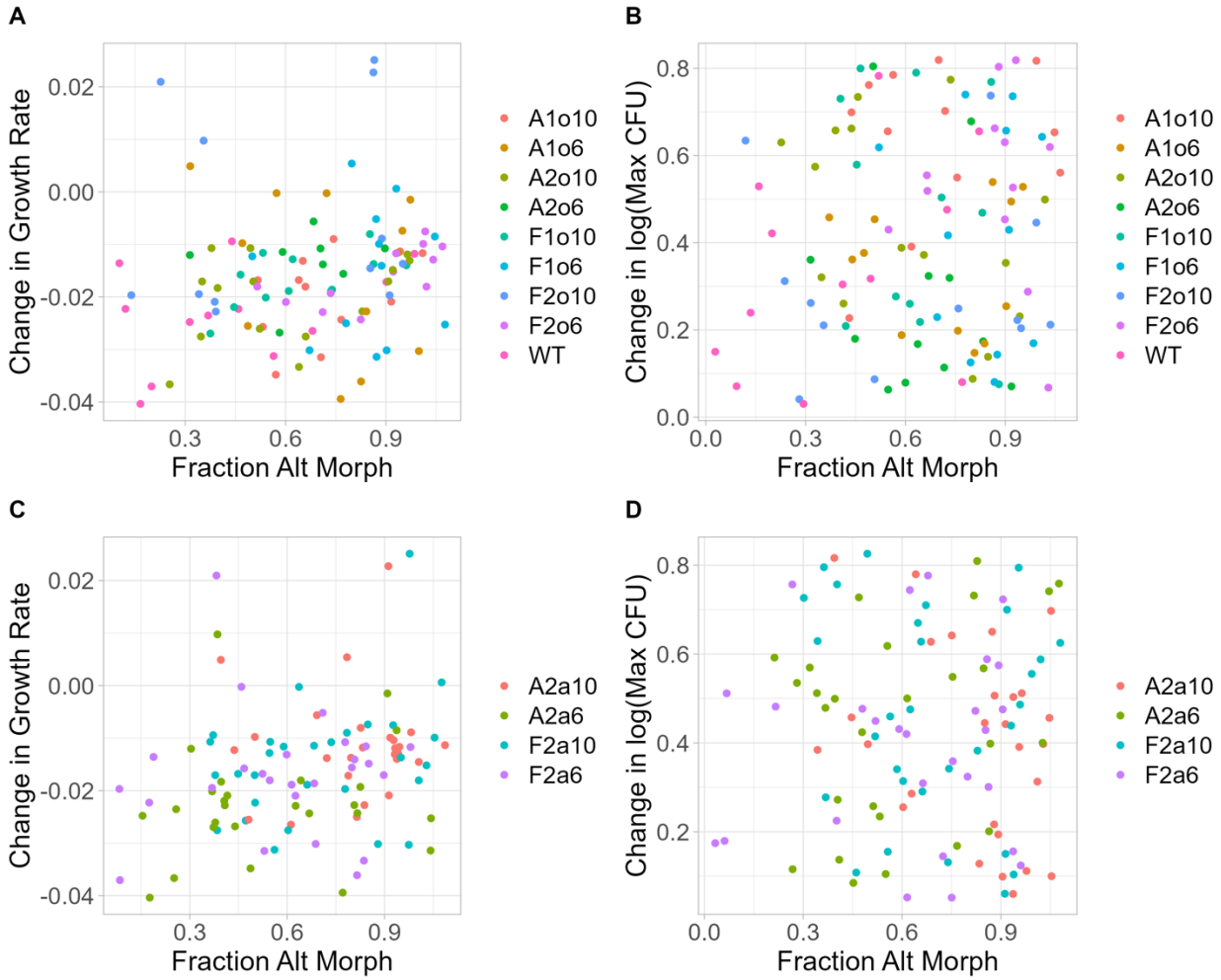

Figure 9. Neither growth rate nor carrying capacity in NGM explain outcomes of pairwise competition. Neither Δr (A, C) nor Δlog(CFU/mL) (B, D) between alternate and original morphs were significantly associated with fraction alternate morph in pairwise competition (linear regression, slopes $p>0.05$). Data are colored by original morph (A, B) and by alternate morph (C, D) to illustrate lack of dependence of these results on community and passage. (Data by Megan Taylor and Marissa Duckett) 14

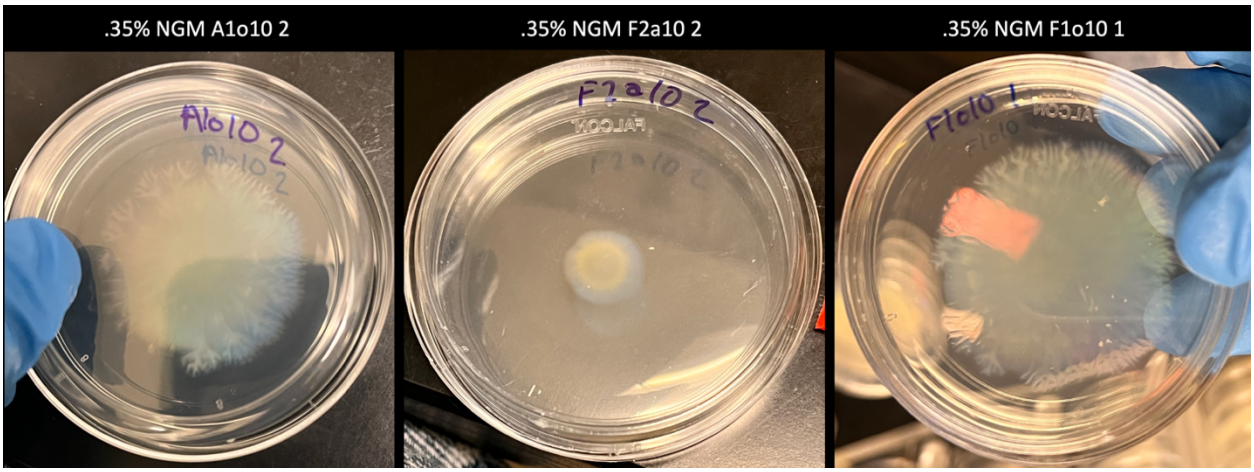

Figure 10. Photographs of iridescence in alternate and original colonies during a surface motility assay on .35% agar NGM plates after 48hrs of growth. 16

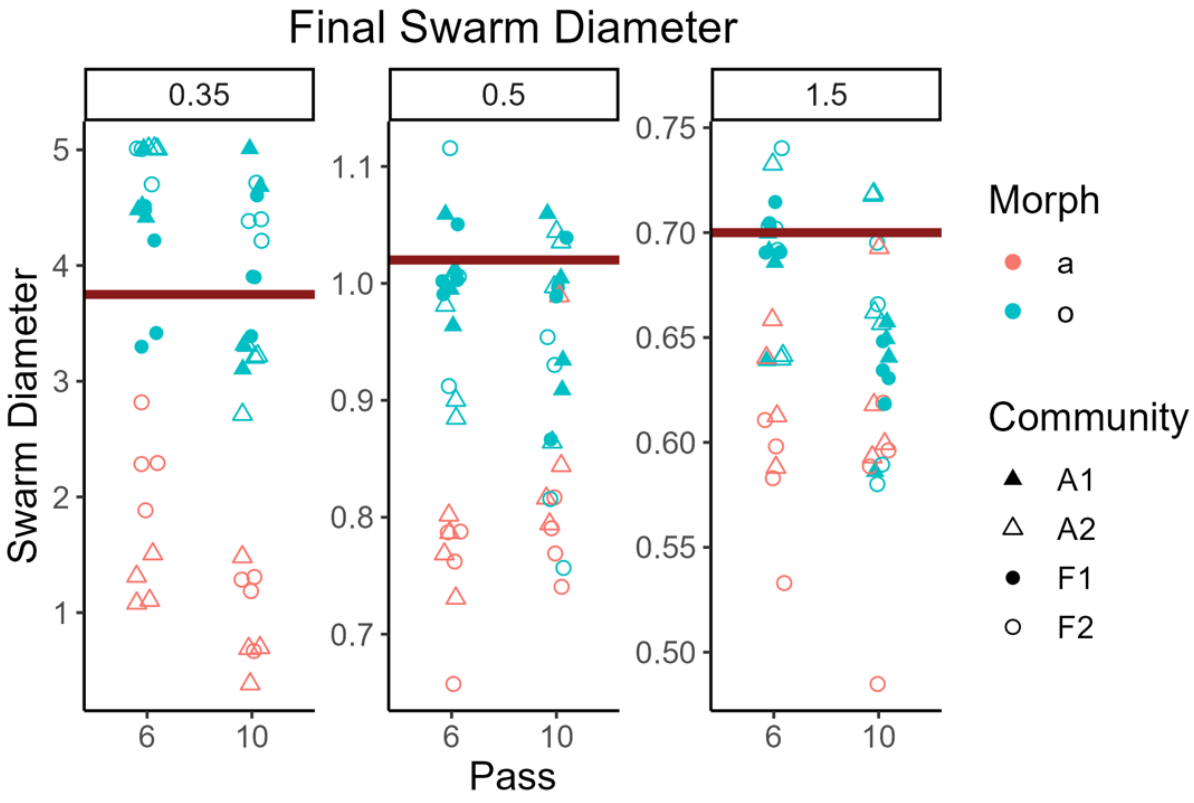

Figure 11. Surface motility of original and alternate morphs of *C. gleum* on 0.35%, 0.5% and 1.5% NGM agar. Diameter of motility in cm is the vertical axis and passage (6 or 10) is the

horizontal axis. The red line represents the median diameter of ancestral colonies on the indicated concentration of agar. Blue points are original morphs, red points are alternate morphs; each shape represents one community and replicate (n=4 isolates from single colony picks for each combination of community, replicate, and passage). 16

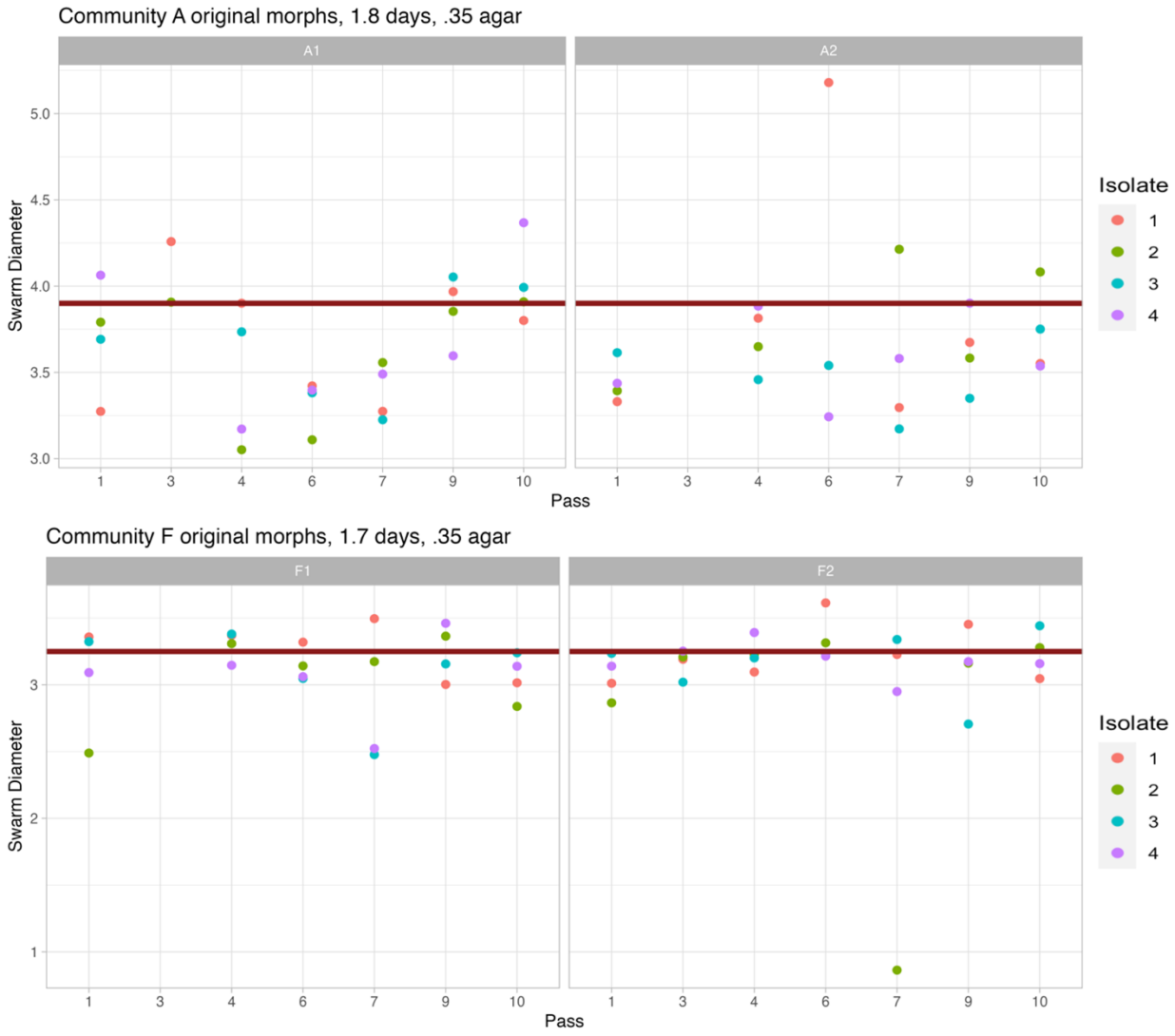

Figure 12. Surface motility of original morphs from passages 1-10 of communities A and F. Isolates from passes 6 and 10 are the same as in the previous figure; all other isolates were retrieved by streaking out glycerol stocks of worm-associated community samples and re-

streaking single colony isolates to confirm morphology (n=4 isolates per community and passage). No isolates were available for passage 2 because no samples were frozen during this passage; glycerol stocks of all pass-8 communities, and of community F1 and A2 in pass 3, did not produce colonies. Note that community-A and community-F isolates were assayed on separate days, with separate batches of agar plates, and the raw diameters cannot be compared across runs due to inherent variability in these assays. 18

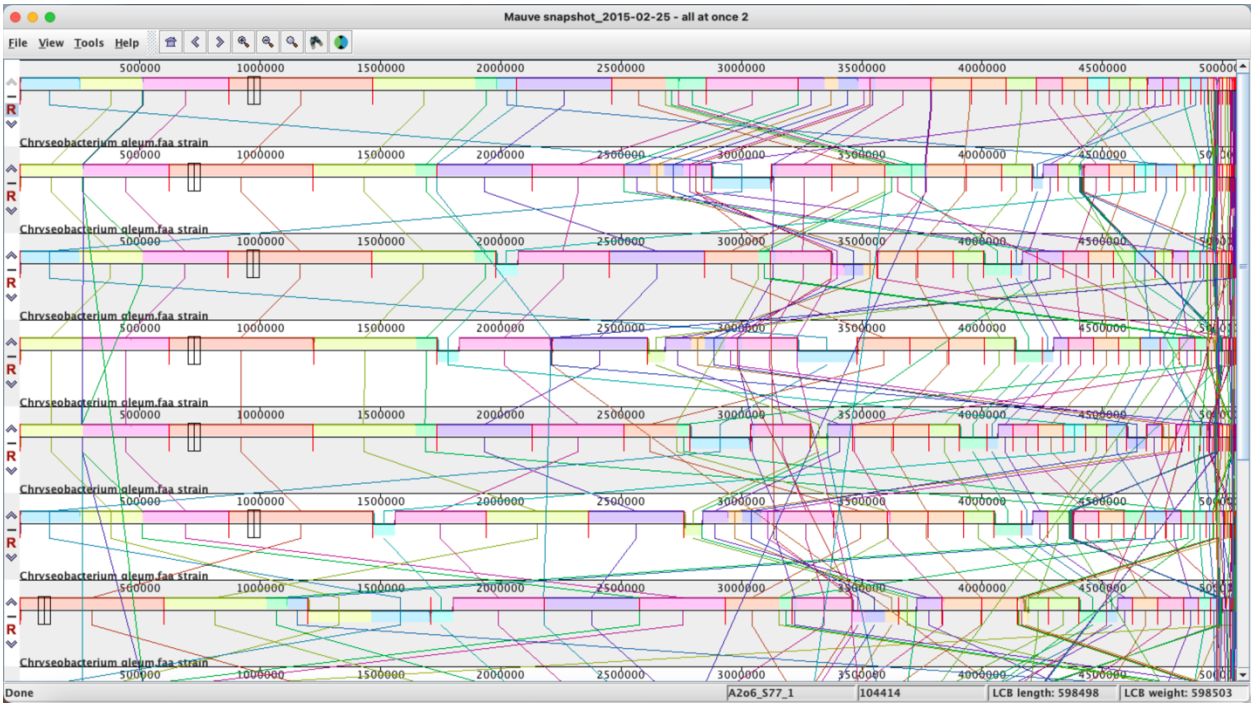

Figure 13. Whole-genome alignment on Mauve. Seven of the eleven sequenced strains are displayed.....21

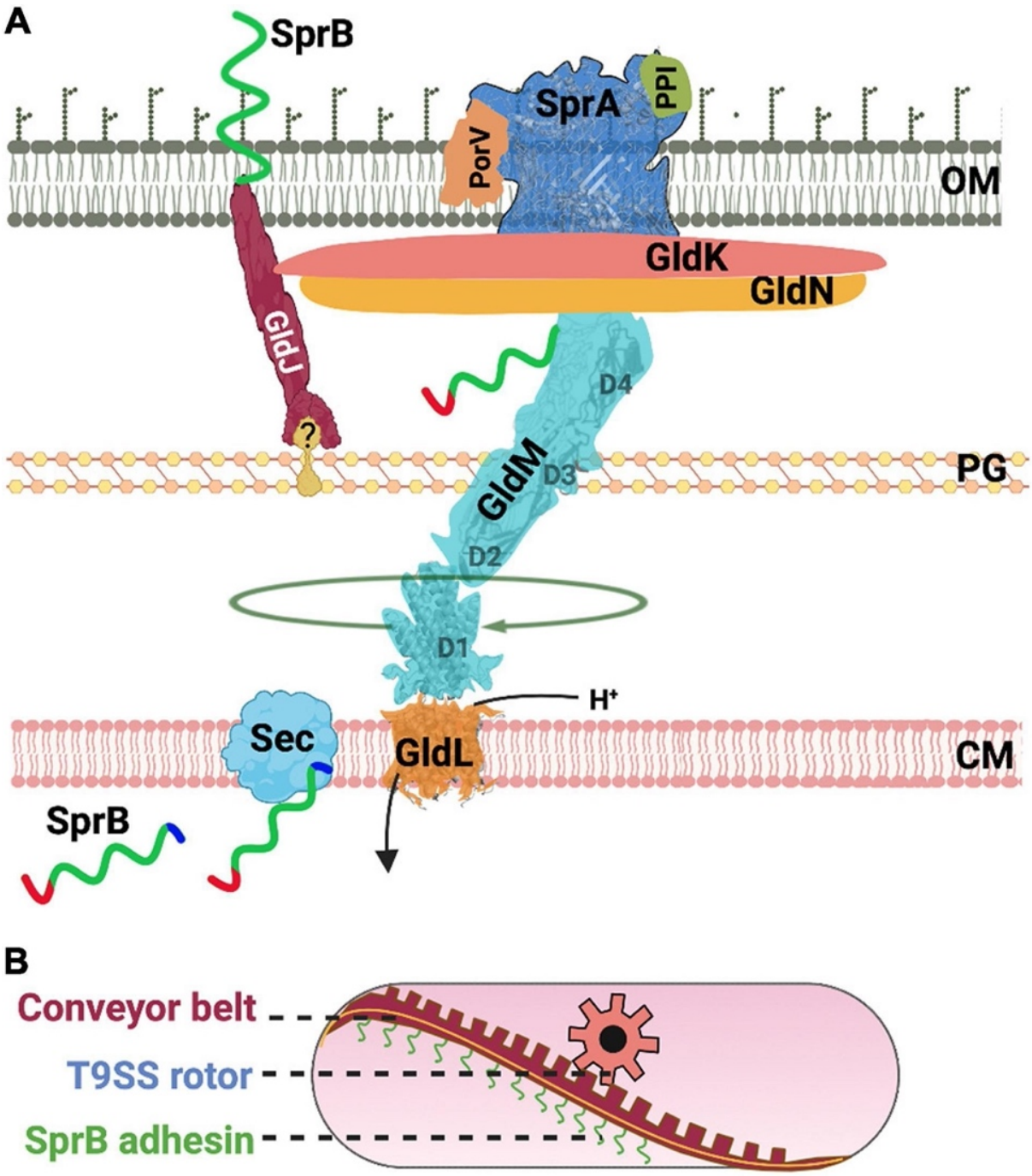

Figure 14. Gliding motility in Flavobacteriales is a function of the Type 9 Secretion System (T9SS). Figure originally published as Figure 2 of (Trivedi et al. 2022), based on the T9SS of *F. johnsoniae* and *P. gingivalis*. The ancestral CG isolate and all other sequenced isolates lack an annotated SprB homolog; in fact, no specific adhesins are annotated on these genomes. These *C. gleum* genomes do show homologs for SprA, PorV, PorP, PorT and all *gld* genes. *gldN, gldM,*

gldL, and *gldK* are adjacent to one another and appear to be a single operon; the same is true for *porV, porU*, and *gldJ,* and for *gldB* and *gldC*. **(A)** A cartoon of the nuts and bolts of the T9SS motor that drives protein secretion and gliding motility. T9SS substrates (SprB shown as an example) are transported to the periplasm *via* the Sec transport pathway. The CTD of T9SS substrates is cleaved during transport. A recent model suggests that the proton channel GldL powers the rotation of T9SS. **(B)** A cartoon of the molecular rack and pinion machinery that drives gliding motility. A model based on recent data suggests that the rotary T9SS pinion drives a cell-surface conveyor belt (rack). Cell-surface adhesins such as SprB are secreted by T9SS and are loaded onto the conveyor belt. Interaction of SprB with an external substratum results in screw-like gliding motility of the bacterial cell.

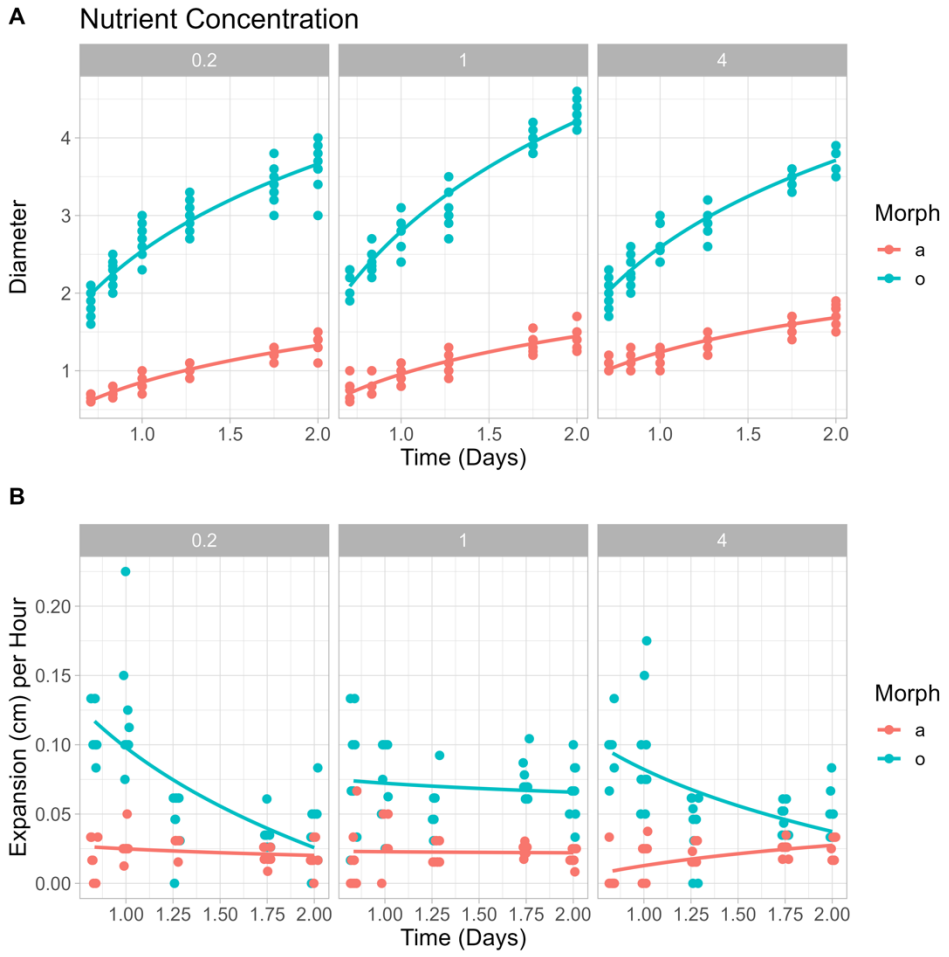

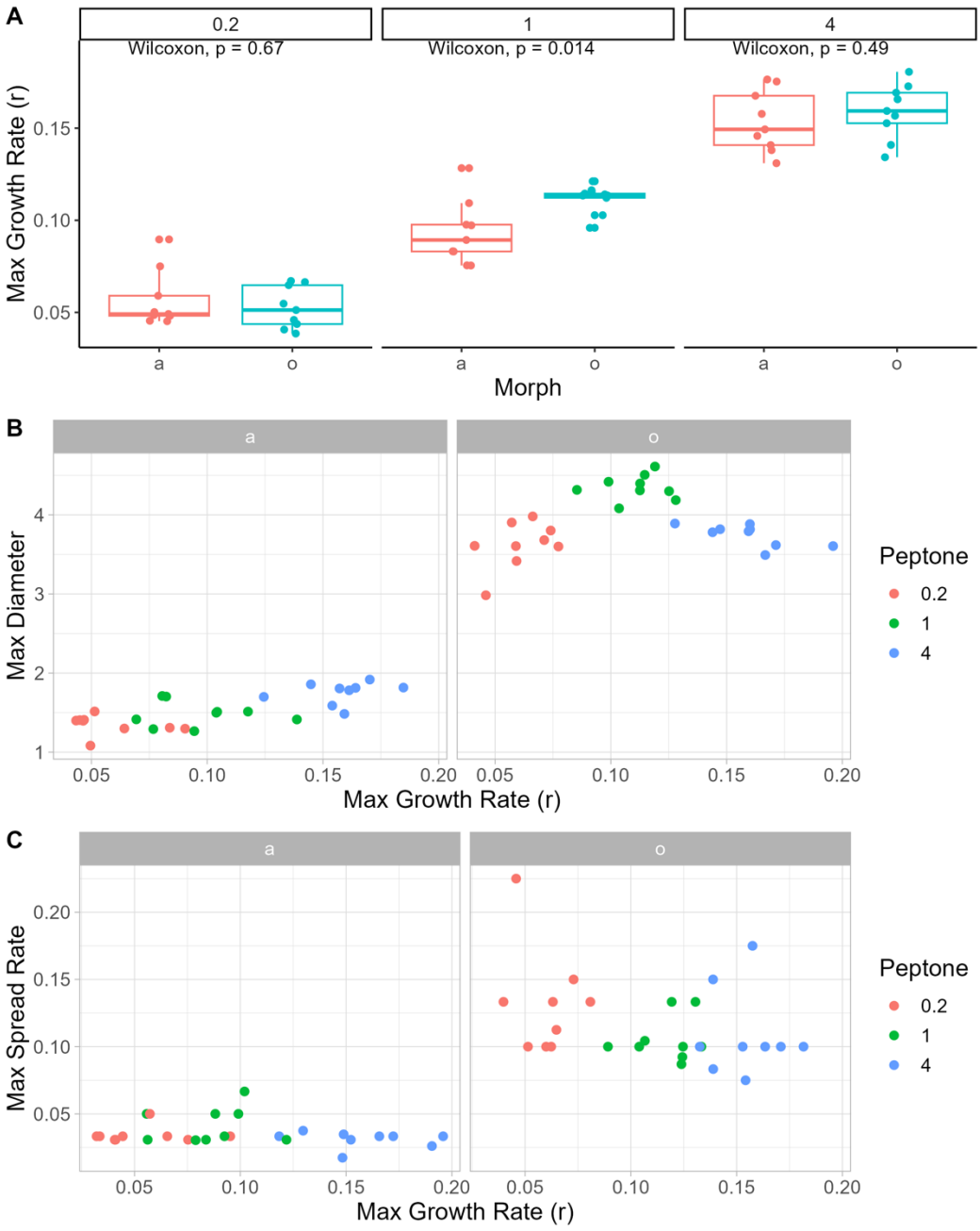

Figure 16. Nutrient concentration alters growth rates, but growth rate does not explain most differences in surface motility. Strains used in these experiments were alternate and original morph isolates from community F2 pass 6 (n=3 isolates per morph, all in technical triplicate; all data points shown). (A) Logistic growth rates were inferred from spline fits to OD600 data when isolates were grown for 24 hours in liquid NGM with 0.25X, 1X or 4X peptone. (B) Logistic growth rates vs maximum diameter (48h growth) on 0.35% NGM plates at each concentration of

peptone. For alternate morphs, max diameter and saturation OD are positively correlated (linear slope = 3.7, p=8.8e-06); for original morphs, there is no statistically significant linear correlation (p=0.4). (C) Logistic growth rate vs maximum surface spreading rate on 0.35% NGM agar at each concentration of peptone. Maximum spreading rate and saturation OD are not significantly linearly correlated for either morph (both p~0.25). 26

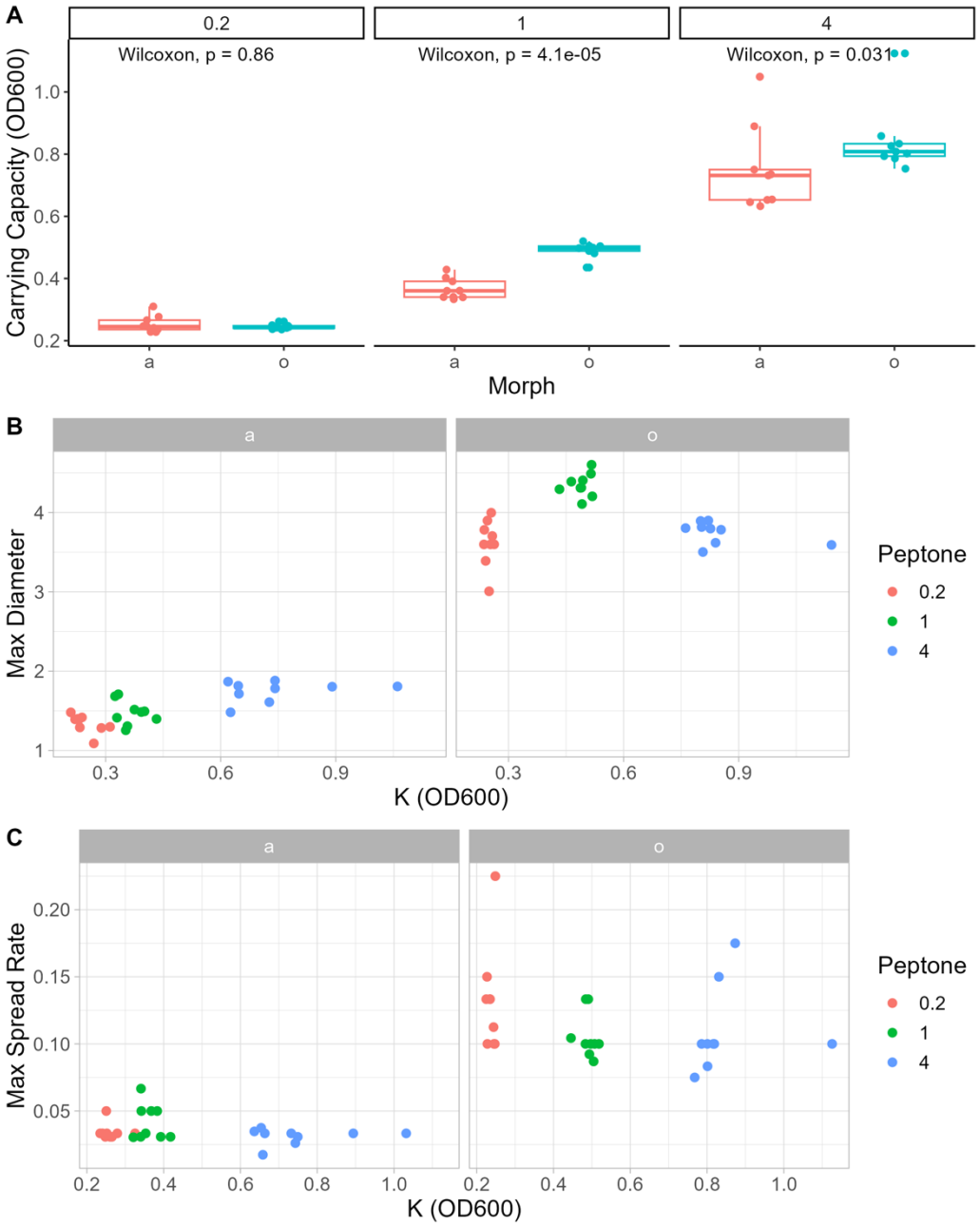

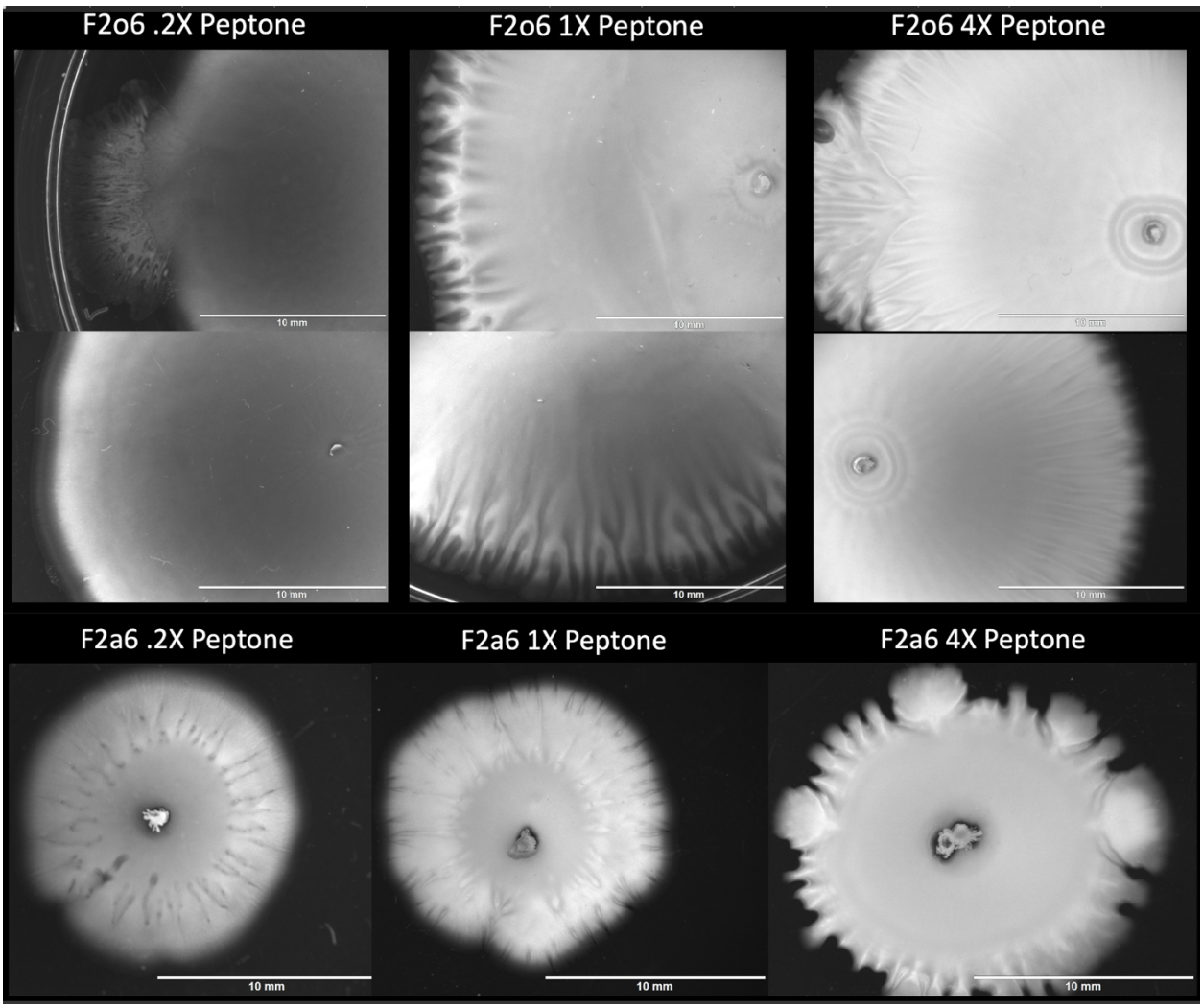

Figure 18. Dark-field microscopy of colony frontiers on 0.35% NGM agar at 48 hours growth. 29

Tables:

Species	Abbreviation
B-2879 *Arthrobacter aurescens*	AA
B-1876 *Bacillus spp.*	BS
B-14798 *Chryseobacterium gleum*	CG
B-14848 *Chryseobacterium indologenes*	CI
B-24236 *Microbacterium oxidans*	MO
ATTC 49188 *Ochrobactrum anthropi*	OA
B-1574 *Rhodococcus erythropolis* (mucoid)	RE15M
B-1574 *Rhodococcus erythropolis* (dry)	RE15D
B-16025 *Rhodococcus erythropolis*	RE16
B-23393 *Sphingobacterium spiritivorum*	SS
B-14902 *Sphingobacterium thalpopium*	ST

Table 1. These species are the eleven *C. elegans*-naïve soil bacterial isolates selected from USDA NRRL soil bacteria collection used to create communities. Three of seven genera (*Chryseobacterium, Rhodococcus, and Sphingobacterium)* are represented by more than one species or isolate..... 35

Bacteria: AA, MO,BS, OA, RE15D, RE15M, RE16, CI, CG, SS, ST							
Multispecies Combinations							
A	AA	MO	RE15D	BS	OA	CG	SS
B	AA	MO	RE15D	BS	OA	CG	ST
C	AA	MO	RE15D	BS	OA	CI	SS
D	AA	MO	RE15D	BS	OA	CI	ST
E	AA	MO	RE15M	BS	OA	CG	SS
F	AA	MO	RE15M	BS	OA	CG	ST
G	AA	MO	RE15M	BS	OA	CI	SS
H	AA	MO	RE15M	BS	OA	CI	ST
I	AA	MO	RE16	BS	OA	CG	SS
J	AA	MO	RE16	BS	OA	CG	ST
K	AA	MO	RE16	BS	OA	CI	SS
L	AA	MO	RE16	BS	OA	CI	ST

Table 2. Combinatorial composition of each of the twelve seven-species starting communities A-L. 36

References

Avershina, E., K. Lundgård, M. Sekelja, C. Dotterud, O. Storrø, T. Øien, R. Johnsen, and K. Rudi. 2016. "Transition from Infant- to Adult-like Gut Microbiota." *Environmental Microbiology* 18 (7): 2226–36. https://doi.org/10.1111/1462-2920.13248.

Blum, Winfried E.H., Sophie Zechmeister-Boltenstern, and Katharina M. Keiblinger. 2019. "Does Soil Contribute to the Human Gut Microbiome?" *Microorganisms* 7 (9): 287. https://doi.org/10.3390/microorganisms7090287.

Chang, Chang-Yu, Jean C. C. Vila, Madeline Bender, Richard Li, Madeleine C. Mankowski, Molly Bassette, Julia Borden, et al. 2021. "Engineering Complex Communities by Directed Evolution." *Nature Ecology & Evolution* 5 (7): 1011–23. https://doi.org/10.1038/s41559-021-01457-5.

Demir, Esin, Y Ilker Yaman, Mustafa Basaran, and Askin Kocabas. 2020. "Dynamics of Pattern Formation and Emergence of Swarming in Caenorhabditis Elegans." Edited by Sandeep Krishna, Aleksandra M Walczak, Vishwesha Guttal, and Davide Marenduzzo. *ELife* 9 (April): e52781. https://doi.org/10.7554/eLife.52781.

Ditmarsch, Dave van, Kerry E. Boyle, Hassan Sakhtah, Jennifer E. Oyler, Carey D. Nadell, Éric Déziel, Lars E. P. Dietrich, and Joao B. Xavier. 2013. "Convergent Evolution of Hyperswarming Leads to Impaired Biofilm Formation in Pathogenic Bacteria." *Cell Reports* 4 (4): 697–708. https://doi.org/10.1016/j.celrep.2013.07.026.

Eckroat, Todd J., Camillus Greguske, and David W. Hunnicutt. 2021. "The Type 9 Secretion System Is Required for Flavobacterium Johnsoniae Biofilm Formation." *Frontiers in Microbiology* 12. https://www.frontiersin.org/articles/10.3389/fmicb.2021.660887.

Estrela, Sylvie, Jean C. C. Vila, Nanxi Lu, Djordje Bajić, Maria Rebolleda-Gómez, Chang-Yu Chang, Joshua E. Goldford, Alicia Sanchez-Gorostiaga, and Álvaro Sánchez. 2021. "Functional Attractors in Microbial Community Assembly." *Cell Systems*, October. https://doi.org/10.1016/j.cels.2021.09.011.

Ford, Suzanne A, and Kayla C King. 2020. "In Vivo Microbial Coevolution Favors Host Protection and Plastic Downregulation of Immunity." *Molecular Biology and Evolution* 38 (4): 1330–38. https://doi.org/10.1093/molbev/msaa292.

Gavriilidou, Asimenia, Johanna Gutleben, Dennis Versluis, Francesca Forgiarini, Mark W. J. van Passel, Colin J. Ingham, Hauke Smidt, and Detmer Sipkema. 2020. "Comparative Genomic Analysis of Flavobacteriaceae: Insights into Carbohydrate Metabolism, Gliding Motility and Secondary Metabolite Biosynthesis." *BMC Genomics* 21 (1): 569. https://doi.org/10.1186/s12864-020-06971-7.

Khare, Devanshi, Pallavi Chandwadkar, and Celin Acharya. 2022. "Gliding Motility of a Uranium-Tolerant Bacteroidetes Bacterium Chryseobacterium Sp. Strain PMSZPI: Insights into the Architecture of Spreading Colonies." *Environmental Microbiology Reports* 14 (3): 453–63. https://doi.org/10.1111/1758-2229.13034.

Louca, Stilianos, Martin F. Polz, Florent Mazel, Michaeline B. N. Albright, Julie A. Huber, Mary I. O'Connor, Martin Ackermann, et al. 2018. "Function and Functional Redundancy in Microbial Systems." *Nature Ecology & Evolution* 2 (6): 936–43. https://doi.org/10.1038/s41559-018-0519-1.

McBride, Mark J. 2014. "The Family Flavobacteriaceae." In *The Prokaryotes: Other Major Lineages of Bacteria and The Archaea*, edited by Eugene Rosenberg, Edward F. DeLong, Stephen Lory, Erko Stackebrandt, and Fabiano Thompson, 643–76. Berlin, Heidelberg: Springer. https://doi.org/10.1007/978-3-642-38954-2_130.

McBride, Mark J., and Yongtao Zhu. 2013. "Gliding Motility and Por Secretion System Genes Are Widespread among Members of the Phylum Bacteroidetes." *Journal of Bacteriology* 195 (2): 270–78. https://doi.org/10.1128/JB.01962-12.

Menon, S. K., and C. M. Lawrence. 2013. "Helix-Turn-Helix Motif." In *Brenner's Encyclopedia of Genetics (Second Edition)*, edited by Stanley Maloy and Kelly Hughes, 412–15. San Diego: Academic Press. https://doi.org/10.1016/B978-0-12-374984-0.00689-6.

Morales-Soto, Nydia, Morgen E. Anyan, Anne E. Mattingly, Chinedu S. Madukoma, Cameron W. Harvey, Mark Alber, Eric Déziel, Daniel B. Kearns, and Joshua D. Shrout. 2015. "Preparation, Imaging, and Quantification of Bacterial Surface Motility Assays." *Journal of Visualized Experiments : JoVE*, no. 98 (April): 52338. https://doi.org/10.3791/52338.

Morella, Norma M., Francis Cheng-Hsuan Weng, Pierre M. Joubert, C. Jessica E. Metcalf, Steven Lindow, and Britt Koskella. 2019. "Successive Passaging of a Plant-Associated Microbiome Reveals Robust Habitat and Host Genotype-Dependent Selection." *Proceedings of the National Academy of Sciences*, December. https://doi.org/10.1073/pnas.1908600116.

Morran, Levi T., Olivia G. Schmidt, Ian A. Gelarden, Raymond C. Parrish, and Curtis M. Lively. 2011. "Running with the Red Queen: Host-Parasite Coevolution Selects for Biparental Sex." *Science (New York, N.y.)* 333 (6039): 216–18. https://doi.org/10.1126/science.1206360.

Natarajan, Vengadesh Perumal, Xinxu Zhang, Yuki Morono, Fumio Inagaki, and Fengping Wang. 2016. "A Modified SDS-Based DNA Extraction Method for High Quality Environmental DNA from Seafloor Environments." *Frontiers in Microbiology* 7 (June): 986. https://doi.org/10.3389/fmicb.2016.00986.

Ottemann, Karen M., and Jeff F. Miller. 1997. "Roles for Motility in Bacterial–Host Interactions." *Molecular Microbiology* 24 (6): 1109–17. https://doi.org/10.1046/j.1365-2958.1997.4281787.x.

Paillat, Maëlle, Ignacio Lunar Silva, Eric Cascales, and Thierry Doan. 2023. “A Journey with Type IX Secretion System Effectors: Selection, Transport, Processing and Activities.” *Microbiology* 169 (4): 001320. https://doi.org/10.1099/mic.0.001320.

Palma, Victoria, María Soledad Gutiérrez, Orlando Vargas, Raghuveer Parthasarathy, and Paola Navarrete. 2022. “Methods to Evaluate Bacterial Motility and Its Role in Bacterial–Host Interactions.” *Microorganisms* 10 (3): 563. https://doi.org/10.3390/microorganisms10030563.

Penttinen, Reetta, Ville Hoikkala, and Lotta-Riina Sundberg. 2018. “Gliding Motility and Expression of Motility-Related Genes in Spreading and Non-Spreading Colonies of Flavobacterium Columnare.” *Frontiers in Microbiology* 9. https://www.frontiersin.org/articles/10.3389/fmicb.2018.00525.

Petit, Robert A., and Timothy D. Read. 2020. “Bactopia: A Flexible Pipeline for Complete Analysis of Bacterial Genomes.” *MSystems* 5 (4): e00190-20. https://doi.org/10.1128/mSystems.00190-20.

Rinninella, Emanuele, Pauline Raoul, Marco Cintoni, Francesco Franceschi, Giacinto Abele Donato Miggiano, Antonio Gasbarrini, and Maria Cristina Mele. 2019. “What Is the Healthy Gut Microbiota Composition? A Changing Ecosystem across Age, Environment, Diet, and Diseases.” *Microorganisms* 7 (1): 14. https://doi.org/10.3390/microorganisms7010014.

Sato, Keiko, Masami Naya, Yuri Hatano, Yoshio Kondo, Mari Sato, Yuka Narita, Keiji Nagano, Mariko Naito, Koji Nakayama, and Chikara Sato. 2021. “Colony Spreading of the Gliding Bacterium Flavobacterium Johnsoniae in the Absence of the Motility Adhesin SprB.” *Scientific Reports* 11 (1): 967. https://doi.org/10.1038/s41598-020-79762-5.

Shrivastava, Abhishek, Joseph J. Johnston, Jessica M. van Baaren, and Mark J. McBride. 2013. “Flavobacterium Johnsoniae GldK, GldL, GldM, and SprA Are Required for Secretion of the Cell Surface Gliding Motility Adhesins SprB and RemA.” *Journal of Bacteriology* 195 (14): 3201–12. https://doi.org/10.1128/JB.00333-13.

Siguier, Patricia, Edith Gourbeyre, and Mick Chandler. 2014. “Bacterial Insertion Sequences: Their Genomic Impact and Diversity.” *FEMS Microbiology Reviews* 38 (5): 865–91. https://doi.org/10.1111/1574-6976.12067.

Simmons, Lyle A., James J. Foti, Susan E. Cohen, and Graham C. Walker. 2008. “The SOS Regulatory Network.” *EcoSal Plus* 2008 (July): 10.1128/ecosalplus.5.4.3. https://doi.org/10.1128/ecosalplus.5.4.3.

Singer, Esther, Bill Andreopoulos, Robert M. Bowers, Janey Lee, Shweta Deshpande, Jennifer Chiniquy, Doina Ciobanu, et al. 2016. “Next Generation Sequencing Data of a Defined Microbial Mock Community.” *Scientific Data* 3 (1): 160081. https://doi.org/10.1038/sdata.2016.81.

Soberón-Chávez, Gloria, Luis D. Alcaraz, Estefanía Morales, Gabriel Y. Ponce-Soto, and Luis Servín-González. 2017. “The Transcriptional Regulators of the CRP Family Regulate Different Essential Bacterial Functions and Can Be Inherited Vertically and Horizontally.” *Frontiers in Microbiology* 8 (May): 959. https://doi.org/10.3389/fmicb.2017.00959.

Steinberg, James P., and Eileen M. Burd. 2015. “238 - Other Gram-Negative and Gram-Variable Bacilli.” In *Mandell, Douglas, and Bennett’s Principles and Practice of Infectious Diseases (Eighth Edition)*, edited by John E. Bennett, Raphael Dolin, and Martin J. Blaser, 2667-2683.e4. Philadelphia: W.B. Saunders. https://doi.org/10.1016/B978-1-4557-4801-3.00238-1.

Stiernagle, Theresa. 2006. “Maintenance of C. Elegans.” Edited by The C. elegans Research Community. *WormBook*, February. https://doi.org/10.1895/wormbook.1.101.1.

Taylor, Megan, Lili Janasky, and Nic Vega. 2022. “Convergent Structure with Divergent Adaptations in Combinatorial Microbiome Communities.” *FEMS Microbiology Ecology* 98 (11): fiac115. https://doi.org/10.1093/femsec/fiac115.

Taylor, Megan, and N. M. Vega. 2021. “Host Immunity Alters Community Ecology and Stability of the Microbiome in a Caenorhabditis Elegans Model.” *MSystems* 6 (2). https://doi.org/10.1128/mSystems.00608-20.

Tremblay, Julien, and Eric Déziel. 2008. “Improving the Reproducibility of Pseudomonas Aeruginosa Swarming Motility Assays.” *Journal of Basic Microbiology* 48 (6): 509–15. https://doi.org/10.1002/jobm.200800030.

Verstraeten, Natalie, Kristien Braeken, Bachaspatimayum Debkumari, Maarten Fauvart, Jan Fransaer, Jan Vermant, and Jan Michiels. 2008. “Living on a Surface: Swarming and Biofilm Formation.” *Trends in Microbiology* 16 (10): 496–506. https://doi.org/10.1016/j.tim.2008.07.004.

Wei, Zhong, Yian Gu, Ville-Petri Friman, George A. Kowalchuk, Yangchun Xu, Qirong Shen, and Alexandre Jousset. 2019. “Initial Soil Microbiome Composition and Functioning Predetermine Future Plant Health.” *Science Advances* 5 (9): eaaw0759. https://doi.org/10.1126/sciadv.aaw0759.